QEX

$1.75

ARRL Experimenter's Exchange

March 1995

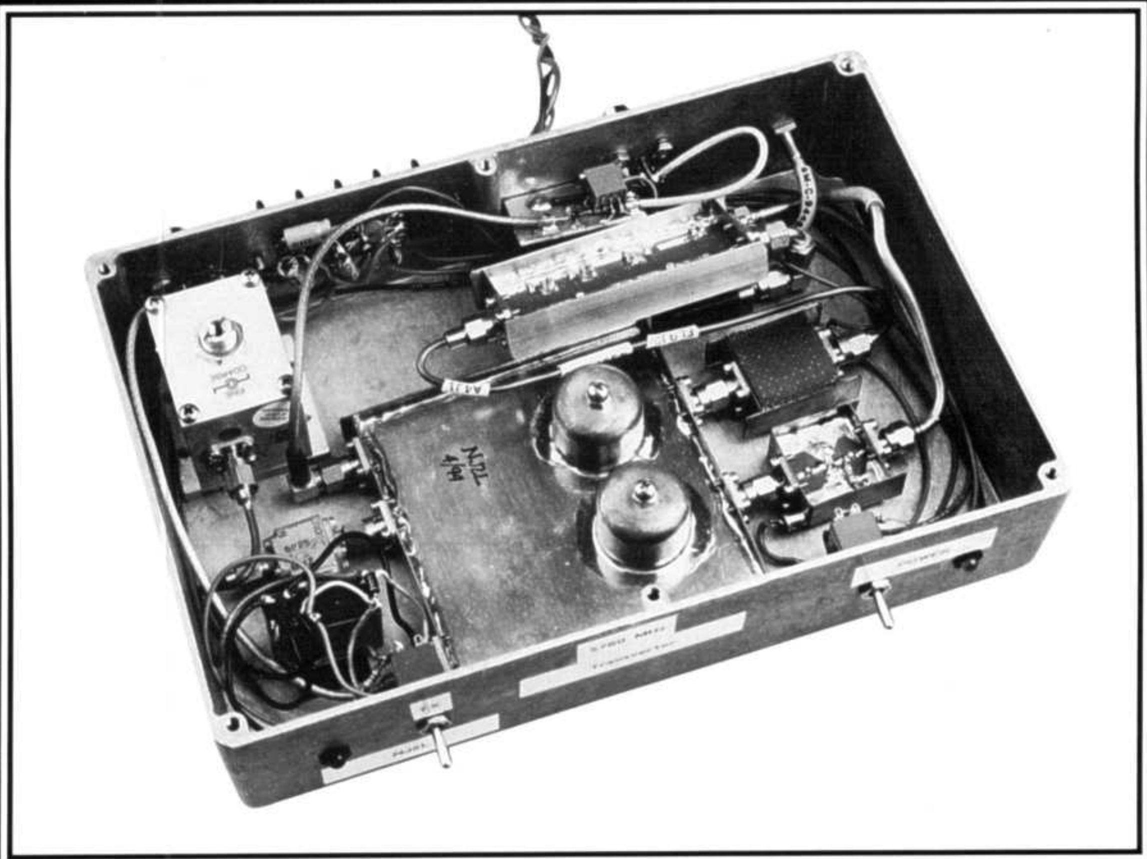

5760 MHz the Modular Way

QEX: The ARRL
Experimenter's Exchange
American Radio Relay League
225 Main Street
Newington, CT USA 06111

QEX (ISSN: 0886-8093 USPS 011-424) is published monthly by the American Radio Relay League, Newington, CT USA.

Second-class postage paid at Hartford, Connecticut and additional mailing offices.

David Sumner, K1ZZ
Publisher

Jon Bloom, KE3Z
Editor

Lori Weinberg
Assistant Editor

Harold Price, NK6K
Zack Lau, KH6CP
Contributing Editors

Production Department

Mark J. Wilson, AA2Z
Publications Manager

Michelle Bloom, WB1ENT
Production Supervisor

Sue Fagan
Graphic Design Supervisor

Joe Costa
Technical Illustrator

Joe Shea
Production Assistant

Advertising Information Contact:

Brad Thomas, KC1EX, *Advertising Manager*
American Radio Relay League
203-667-2494 direct
203-666-1541 ARRL
203-665-7531 fax

Circulation Department

Debra Jahnke, *Manager*
Kathy Fay, N1GZO, *Deputy Manager*
Cathy Stepina, *QEX Circulation*

Offices

225 Main St, Newington, CT 06111-1494 USA
Telephone: 203-666-1541
Telex: 650215-5052 MCI
FAX: 203-665-7531 (24 hour direct line)
Electronic Mail: MCIMAILID: 215-5052
Internet:qex@arrl.org

Subscription rate for 12 issues:

In the US: ARRL Member $12, nonmember $24;

US, Canada and Mexico by First Class Mail: ARRL Member $25, nonmember $37;

Elsewhere by Surface Mail (4-8 week delivery): ARRL Member $20, nonmember $32;

Elsewhere by Airmail: ARRL Member $48, nonmember $60.

QEX subscription orders, changes of address, and reports of missing or damaged copies may be marked: *QEX* Circulation. Postmaster: Form 3579 requested. Send change of address to: American Radio Relay League, 225 Main St, Newington, CT 06111-1494.

Members are asked to include their membership control number or a label from their *QST* wrapper when applying.

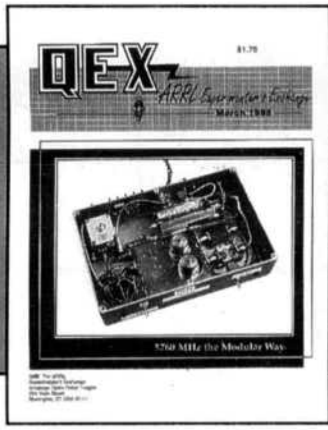

About the Cover

NJ2L's modular 5760-MHz transverter can be built using readily available parts and designs.

ISSUE NO. 157

Features

Columns

March 1995 QEX Advertising Index

THE AMERICAN RADIO RELAY LEAGUE

The American Radio Relay League, Inc, is a noncommercial association of radio amateurs, organized for the promotion of interests in Amateur Radio communication and experimentation, for the establishment of networks to provide communications in the event of disasters or other emergencies, for the advancement of radio art and of the public welfare, for the representation of the radio amateur in legislative matters, and for the maintenance of fraternalism and a high standard of conduct.

ARRL is an incorporated association without capital stock chartered under the laws of the state of Connecticut, and is an exempt organization under Section 501(c)(3) of the Internal Revenue Code of 1986. Its affairs are governed by a Board of Directors, whose voting members are elected every two years by the general membership. The officers are elected or appointed by the Directors. The League is noncommercial, and no one who could gain financially from the shaping of its affairs is eligible for membership on its Board.

"Of, by, and for the radio amateur, "ARRL numbers within its ranks the vast majority of active amateurs in the nation and has a proud history of achievement as the standard-bearer in amateur affairs.

A bona fide interest in Amateur Radio is the only essential qualification of membership; an Amateur Radio license is not a prerequisite, although full voting membership is granted only to licensed amateurs in the US.

Membership inquiries and general correspondence should be addressed to the administrative headquarters at 225 Main Street, Newington, CT 06111 USA.

Telephone: 203-666-1541
Telex: 650215-5052 MCI
MCIMAIL (electronic mail system) ID: 215-5052
FAX: 203-665-7531 (24-hour direct line)

Officers

President: GEORGE S. WILSON III, W4OYI
1649 Griffith Ave, Owensboro, KY 42301

Executive Vice President: DAVID SUMNER, K1ZZ

Purpose of *QEX*:

1) provide a medium for the exchange of ideas and information between Amateur Radio experimenters
2) document advanced technical work in the Amateur Radio field
3) support efforts to advance the state of the Amateur Radio art

All correspondence concerning *QEX* should be addressed to the American Radio Relay League, 225 Main Street, Newington, CT 06111 USA. Envelopes containing manuscripts and correspondence for publication in *QEX* should be marked: Editor, *QEX*.

Both theoretical and practical technical articles are welcomed. Manuscripts should be typed and doubled spaced. Please use the standard ARRL abbreviations found in recent editions of *The ARRL Handbook*. Photos should be glossy, black and white positive prints of good definition and contrast, and should be the same size or larger than the size that is to appear in *QEX*.

Any opinions expressed in *QEX* are those of the authors, not necessarily those of the editor or the League. While we attempt to ensure that all articles are technically valid, authors are expected to defend their own material. Products mentioned in the text are included for your information; no endorsement is implied. The information is believed to be correct, but readers are cautioned to verify availability of the product before sending money to the vendor.

Empirically Speaking

Licensed to Experiment

Maybe we've been spending too much time lately on the Internet and the on-line subscription services, but we've noticed an ongoing debate about "upgrading" within Amateur Radio. The thesis of the argument seems to be that the diminishing percentage of higher-class licenses indicates that amateurs are less technically adept than they once were. The reason the percentages are changing, of course, is the influx of new amateurs who get a Technician license and keep it.

We're puzzled by the outrage some feel over this trend, particularly when their argument is that it indicates a lowering of amateur technical abilities. It's just not clear that there is any particular correlation between the class of license one holds and one's technical ability.

What motivates a holder of a Technician license to get a General, Advanced or Amateur Extra license? Aside from the ego trip of having the highest license class possible, the only reasonable motivation is to gain access to the additional privileges conveyed by those licenses. The major additional privilege of licenses above Technician is access to all of the MF and HF amateur bands and modes, and that comes with the General Class license. License classes higher than General only expand the allowed spectrum.

The point is, an amateur wanting to experiment or develop technical skills and knowledge doesn't need a license higher than Technician Class unless he wants access to the HF bands. There is plenty of grist for the experimental mill at VHF and above; some amateurs will never use HF or feel the lack of HF privileges. And even if HF is the chosen experimental ground, there is nothing you can do with an Advanced or Amateur Extra that you can't do with a General—you can just do it in more places. So, where is the motivational tie-in between exercising technical skills and license class?

Amateurs of all license classes can and do contribute to amateur technical activities. That those with higher-class licenses are more capable of doing so is an unproven assumption. What *is* clear is that a Technician license gives plenty of scope for experimentation, and it's our observation that experimentation is alive and well among the Technician ranks.

This Month in *QEX*

The directional coupler is an integral part of many SWR meters, but it has other useful applications. William E. Sabin, WØIYH, details how these devices work in "The Lumped-Element Directional Coupler."

5760-MHz is a hot band! *QEX* has brought you equipment designs for this band previously, but "A Modular, High-Performance 5.76-GHz Transverter," by Rus Healy, NJ2L, is the simplest yet to duplicate.

The ARRL Lab has been "Measuring 9600-Baud Radio BER Performance." Find out how it's done in this month's article by Jon Bloom, KE3Z.

Finally, Zack Lau, KH6CP, takes up the difficult question of determining the power limits of circuits containing toroid inductors in this month's "RF" column. His approach makes the calculations quite straightforward.—*KE3Z, email: jbloom@arrl.org (Internet)*

The Lumped-Element Directional Coupler

A thorough analysis and simulation reveal the characteristics of widely used directional couplers.

By William E. Sabin, WØIYH

The use of the two-transformer directional coupler in transmitter directional wattmeter applications is well known in the amateur radio community. The circuit of Fig 1 is typical and is well described elsewhere.[1,2] The FORWARD and REFLECTED outputs are often rectified and the dc output meter is calibrated in terms of power, SWR or return loss.

The advantage of this design is that, if done properly, the meter calibration holds quite well over at least a 20-to-1 frequency range without readjustment, as compared to some previous types, in particular the "Monimatch." (See Notes 1 and 3 for details.)

These couplers, without the rectifiers, are widely used as instrumentation for various RF measurements, especially in scalar and vector network analyzers of one kind or another, and in phase sensing applications such as automatic antenna tuning networks and feedforward amplifiers.[4,5] In other equipment designs they are used to inject a signal into or to sample a signal from a coaxial cable circuit in various ways. They are also useful in

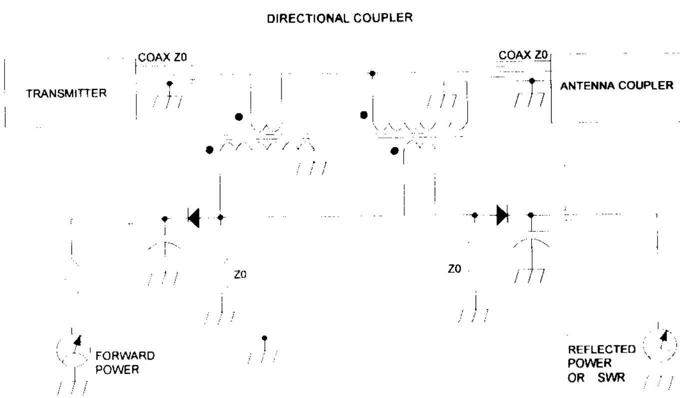

Fig 1—Typical application of a directional coupler as a transmit forward and reflected power meter.

[1]Notes appear on page 11.

1400 Harold Dr SE
Cedar Rapids, IA 52403

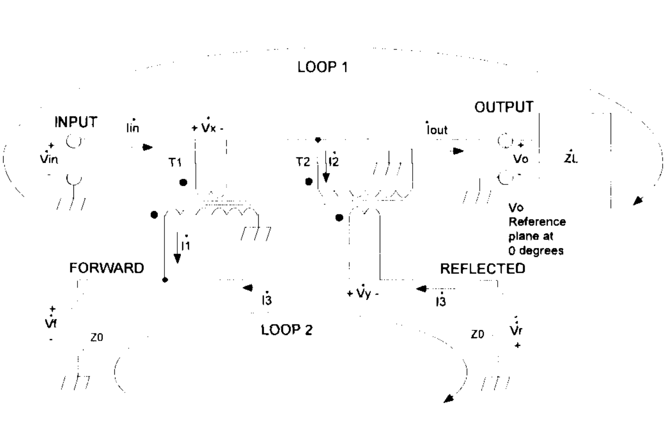

Fig 2—Analysis diagram of a directional coupler.

simple experimental setups in the amateur's home laboratory. They are available in a wide variety of forms from various manufacturers. They are also very easy to construct using simple materials.

The purpose of this *QEX* article is to analyze in detail the behavior and design considerations of the directional coupler. A companion article being prepared for *QST* will describe the construction of some home-built couplers and their usage in some Amateur Radio experiments.

Lumped circuit analysis

The merit of this simplifed mathematical analysis is that it establishes a baseline from which to evaluate simulation and hardware results. It also improves our understanding of the operation of these devices.

If we regard the coupler as a simplified lumped element circuit, disregarding for the moment the concepts of forward and reflected waves, we can gain considerable insight. Fig 2 shows the circuit, with a "reference plane" voltage V_o , at 0° phase, present at the output. A complex load, R_L and X_L in *parallel*, is connected to the output:

$$\dot{Z}_L = \frac{1}{\frac{1}{R_L} + \frac{1}{jX_L}} \qquad \text{Eq 1}$$

where the dot over $\dot{Z}_L$ (and in subsequent usage) indicates a complex quantity. The two identical transformers are assumed for the moment to be ideal at all frequencies. Lead lengths and stray capacitances are ignored.

An examination of Fig 2 shows that:

- Because of symmetry, the INPUT-OUTPUT pair of terminals and the FORWARD-REFLECTED pair are interchangeable and also reversible.
- The INPUT and OUTPUT terminals are isolated from the FORWARD and REFLECTED terminals by T1 and T2, which can be an important instrumentation factor.
- The step-down ratio of the transformers means that the FORWARD and REFLECTED terminals place a light loading, or *burden*, on the INPUT-OUTPUT path. The coupler can be a permanent part of the equipment with almost no degradation of system performance.

T1 produces a current $\dot{I}_1$ which is proportional to the input current $\dot{I}_{in}$. T2 produces a voltage $\dot{V}_y$ which is proportional to the output voltage V_o. $\dot{I}_1$ and $\dot{V}_y$ combine to produce voltages $\dot{V}_f$ and $\dot{V}_r$ with the peak-of-sine-wave polarities shown. If $\dot{V}_f$ and $\dot{V}_y$ are exactly equal in amplitude and phase, then $\dot{V}_r = 0$. That is, $\dot{I}_3 = 0$.

An examination of the circuit shows that two main loop equations can be written along the paths indicated in Fig 2.

$$-\dot{V}_{in} + \dot{V}_x + V_o = 0 \qquad \text{Eq 2}$$

$$-\dot{V}_f + \dot{V}_y - \dot{V}_r = 0 \qquad \text{Eq 3}$$

If $\dot{V}_{in}$ is specified then there are five unknowns in these two equations. The load impedance $\dot{Z}_L$ and Z_0, the characteristic impedance of the system (eg, 50 Ω, pure resistance), are both specified. The following auxiliary equations can be substituted in Eqs 2 and 3 to obtain two equations with unknowns $\dot{V}_f$ and $\dot{V}_r$, the voltages at the forward and reflected ports. In these equations N is the turns ratio of T1 and T2.

$$\dot{V}_x = \frac{\dot{V}_f}{N}$$

$$\dot{V}_y = \frac{V_o}{N}$$

$$\dot{I}_1 = \frac{\dot{I}_{in}}{N}$$

$$\text{ie,} \dot{V}_x \dot{I}_{in} = \dot{V}_f \dot{I}_1 = N \dot{V}_x \dot{I}_1 \quad \text{(ideal transformer)}$$

$$\dot{I}_3 = N\,\dot{I}_2$$

$$\text{ie,} V_o \dot{I}_2 = \dot{V}_y \dot{I}_3 = \frac{V_o \dot{I}_3}{N} \quad \text{(ideal transformer)} \qquad \text{Eq 4}$$

$$\dot{V}_r = \dot{I}_3\,Z_0$$

$$\dot{V}_f = \left(\dot{I}_1 + \dot{I}_3\right) Z_0$$

$$\dot{I}_o = \dot{I}_{in} - \dot{I}_2$$

$$\dot{V}_{in} = \dot{V}_x + V_o$$

$$V_o = \dot{I}_o\,\dot{Z}_L$$

The results are as follows:

$$\frac{\dot V_f}{\dot V_{in}} = \frac{N + \frac{\dot Z_L}{Z_0}\left(\frac{N^2+1}{N}\right)}{\dot\Delta}$$

$$\frac{\dot V_r}{\dot V_{in}} = \frac{N\left(1-\frac{\dot Z_L}{Z_0}\right)}{\dot\Delta} \qquad \text{Eq 5}$$

$$\dot\Delta = 1+\frac{\dot Z_L}{Z_0}\left(\frac{2N^4+2N^2+1}{N^2}\right)$$

If $\dot Z_L$ is a pure resistance equal to Z_0 then $\dot V_r = 0$. This happens only when $\dot V_f$ is exactly equal to and in phase with $\dot V_y$, and this in turn occurs only when $\dot Z_L$ is a pure resistance. The complicated nature of these equations suggests the rather involved interactions between T1 and T2: they "talk" to each other.

The voltage $\dot V_r$ is a measure of the relationship between the *current into* $\dot Z_L$ and the *voltage across* $\dot Z_L$. If the complex ratio of voltage to current is not equal to Z_0 then $\dot V_r$ is not zero. The coupler circuit is thus basically an impedance bridge. $\dot Z_L$ at its immediate output terminal can be (and often are) lumped elements of L, C and R or the input terminal of a transmission line.

Interesting information is available from these equations for the special case when $\dot Z_L = Z_0$. The complex input impedance is:

$$\dot Z_{in} = \frac{\dot V_{in}}{\dot I_{in}} = \frac{\dot Z_L}{1-\frac{1}{N}\left(\frac{\dot V_f}{\dot V_{in}} - \frac{\dot Z_L}{Z_0}\frac{\dot V_r}{\dot V_{in}}\right)} \qquad \text{Eq 6}$$

If $\dot Z_L = Z_0$ then $\dot V_r = 0$, and

$$\dot Z_{in} = R_{in} = Z_0\left(\frac{N^2+1}{N^2}\right) \qquad \text{Eq 7}$$

For example, if $N = 10$ and $Z_0 = 50$ then $R_{in} = 50.5$. If $N = \sqrt{10}$ then $Z_{in} = 55.0$, which says that when the coupler is driven from a Z_0 signal generator resistance there is a mismatch loss at the coupler input. This error is quite small for $N \geq 10$.

Eq 5 assumes that $\dot Z_L$ is known and finds $\dot V_f$ and $\dot V_r$ (we will need this later on). But the usual case is that these voltages are measured and the value of $\dot Z_L$ is desired. If Eq 5 is solved for $\dot Z_L$ the result is:

$$\dot Z_L = Z_0\left[\frac{1-\frac{\dot V_r}{\dot V_f}}{1+\frac{\dot V_r}{\dot V_f}\left(\frac{N^2+1}{N^2}\right)}\right]$$

$$\approx Z_0\left[\frac{1-\frac{\dot V_r}{\dot V_f}}{1+\frac{\dot V_r}{\dot V_f}}\right] \text{ if } N \text{ is large} \qquad \text{Eq 8}$$

From this we can see that the coupler can also be an impedance *measuring* device.

The coupler in Fig 2 can also be used in the reverse direction (output V_o and input $\dot V_{in}$ interchanged). An analysis similar to the previous one provides the following equations:

$$\frac{\dot V_f}{\dot V_{in}} = -1\cdot\frac{N\left(\frac{\dot Z_L}{Z_0}+1\right)+\frac{1}{N}}{\dot\Delta}$$

$$\frac{\dot V_r}{\dot V_{in}} = \frac{N\left(\frac{\dot Z_L}{Z_0}-1\right)}{\dot\Delta} \qquad \text{Eq 9}$$

$$\dot\Delta = 2N^2\frac{\dot Z_L}{Z_0}+1$$

The $\dot V_f$ and $\dot V_r$ functions in Fig 2 are interchanged. The results using Eqs 5 and 9 agree within 1% when $N \geq 10$ and only within 10% when $N = \sqrt{10}$. Both agree within 0.1% with their values reported by circuit simulation programs, as we'll see. In the reverse connection there are some phase polarity flips for $\dot V_f$ and $\dot V_r$, as Eq 9 shows.

If Eq 9 is solved for $\dot Z_L$ the result is:

$$\dot Z_L = Z_0\left[\frac{1-\frac{\dot V_r}{\dot V_f}\left(\frac{N^2+1}{N^2}\right)}{1+\frac{\dot V_r}{\dot V_f}}\right]$$

$$\approx Z_0\left[\frac{1-\frac{\dot V_r}{\dot V_f}}{1+\frac{\dot V_r}{\dot V_f}}\right] \text{ if } N \text{ is large} \qquad \text{Eq 10}$$

If $N = 10$, the forward connection and reverse connection results are very close (within 1.0%), especially if $\dot V_r$ is small.

The complex power input $\dot{P}_{in}$ to the coupler involves the input voltage $\dot{V}_{in}$ and $\dot{Z}_{in}$, which is the parallel combination of resistance R_{in} and reactance X_{in}:

$$\dot{P}_{in} = \frac{\dot{V}_{in}^{\,2}}{Z_{in}} = \frac{\left|\dot{V}_{in}^{\,2}\right|}{R_{in}}\Bigg|_{\text{if } \dot{Z}_L = Z_0} \qquad \text{Eq 11}$$

Note that $\dot{V}_f$ and $\dot{V}_r$ respond to *complex* power $\dot{P}_{in}$. The power in the $\dot{V}_f$ port is:

$$P_f = \frac{\left|\dot{V}_f\right|^2}{Z_0} \qquad \text{Eq 12}$$

The coupling factor (CF) is usually defined from the Input port to the Forward port as:

$$\text{CF} = \frac{P_f}{\dot{P}_{in}} = \frac{\left|\dot{V}_f\right|^2 / Z_0}{\dot{V}_{in}^{\,2} / \dot{Z}_{in}} = \frac{1}{N^2+1}\Bigg|_{\text{if } \dot{Z}_L = Z_0}$$

$$\frac{\left|\dot{V}_f\right|}{\left|V_{in}\right|} = \frac{1}{\sqrt{N^2+1}}\Bigg|_{\text{if } \dot{Z}_L = Z_0} \qquad \text{Eq 13}$$

This coupling factor in dB is approximately, but not exactly, equal to –20 log N, where N is the turns ratio of T1 and T2. For example, a 40-turn secondary and 1-turn primary, as in a 1500-W transmitter SWR meter, is nominally a –32 dB coupler, and 0.95 W will be delivered to the FORWARD terminal. If CF is defined from the OUTPUT port to the FORWARD port, as it sometimes is, it is just $1/N^2$.

If $\dot{Z}_L = Z_0$, the ratios of output voltage and power to input voltage and power, with all voltages at reference phase, are:

$$\frac{V_o}{V_{in}} = 1 - \frac{V_f}{NV_{in}} = \frac{N^2}{N^2+1} \qquad \text{Eq 14}$$

$$\frac{P_o}{P_{in}} = \frac{V_o^{\,2} / Z_0}{V_{in}^{\,2} / R_{in}} = \frac{N^2}{N^2+1} \qquad \text{Eq 15}$$

From Eqs 13 and 15 you can see that the sum of the output power and the coupled power is exactly equal to the input power. If $\dot{V}_r$ is not zero for any reason, then the power at the REFLECTED port must be included in the sum, and the equality is still valid.

In Fig 2, if $\dot{V}_{in}$ and $\dot{Z}_L$ are interchanged, the FORWARD terminal reads the value of $\dot{V}_r$. The difference, in dB, between $\dot{V}_f$ and $\dot{V}_r$, if $\dot{Z}_L = Z_0$, is called the *directivity*. In Eqs 5 and 9 this value is infinite if $\dot{Z}_L = Z_0$. In practice, system errors, internal phase shifts and other imperfections of one kind or another limit the directivity to the usual range of 20 to 40 dB. The usual commercial practice is to use an internal resistor at the $\dot{V}_r$ terminal, microstrip circuitry and possibly some small compensating components to improve the directivity. Fig 3 shows how two such couplers are connected back-to-back in order to get maximum directivity for simultaneous forward and reflected measurements. If a single coupler is used, the $\dot{V}_f$ and $\dot{V}_r$ terminals should both be terminated accurately with the Z_0 resistance (Note: coax cables *vary* in their Z_0 values). The two-coupler approach is preferable in more critical applications.

In some interesting applications the REFLECTED port is used as a *second* input port. The power applied to this port phase-combines, at the OUTPUT port, with the signal that is applied to the normal INPUT port. At the same time the REFLECTED port is *isolated* from the INPUT port (but not from a signal that is applied to the the OUTPUT port) *if* the OUTPUT port is terminated with Z_0. The feed-forward amplifier is a good example of this usage.[5]

Forward and reflected wave motions

Directional couplers are often used in coaxial cable circuits where transmission-line wave properties such as standing wave ratio (SWR), forward power, reflected power, reflection coefficient and return loss are the desired measurements. All of these are found directly from the complex ratio $\dot{Z}_L/Z_0$. Only the values of V_o (for power measurements), $\dot{V}_f$, $\dot{V}_r$, N and the Z_0 of the transmission line at the output terminal (assumed to be identical to the Z_0 resistors in Fig 2) are needed to determine these quantities with good accuracy.

The voltage and current at the output terminal of the coupler can be viewed as having forward moving (incident) and backward moving (reflected) wave components as follows—even if the lead lengths are zero:

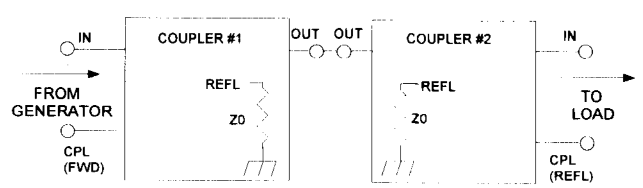

Fig 3—Two directional couplers back-to-back improve directivity.

$$V_o = \dot{V}_o^{\,+} + \dot{V}_o^{\,-}$$

$$\dot{I}_o = \dot{I}_o^{\,+} - \dot{I}_o^{\,-} = \frac{1}{Z_0}\left(\dot{V}_o^{\,+} - \dot{V}_o^{\,-}\right) \qquad \text{Eq 16}$$

These are the solutions, at $x = 0$, to a pair of differential equations for a lossless transmission line with distributed series L and distributed shunt C, where x in this case is the distance from the transmitting end of the line (the end that is connected to the coupler output). If we divide these two equations we get:

$$\frac{V_o}{\dot{I}_o} = \dot{Z}_L = Z_0\frac{1+\dfrac{\dot{V}_o^{\,-}}{\dot{V}_o^{\,+}}}{1-\dfrac{\dot{V}_o^{\,-}}{\dot{V}_o^{\,+}}} = Z_0\frac{1+\dot{\Gamma}}{1-\dot{\Gamma}}$$

$$\approx Z_0\left[\frac{1-\dfrac{\dot{V}_r}{\dot{V}_f}}{1+\dfrac{\dot{V}_r}{\dot{V}_f}}\right] \quad \text{if } N \text{ is large} \qquad \text{Eq 17}$$

In this equation the complex reflection coefficient $\dot{\Gamma}$ is the ratio of the reflected voltage (or current) wave to the incident voltage (or current) wave. If we compare this equation with Eqs 8 and 10 we see a very close similarity if N is large. (Note the plus and minus sign differences; this is a characteristic of the coupler that causes no difficulty.) $\dot{V}_r$ and $\dot{V}_f$ are related to $\dot{V}_o^{\,-}$ and $\dot{V}_o^{\,+}$. If we solve Eq 17 for $\dot{\Gamma}$ the result is:

$$\dot{\Gamma} = \frac{\dfrac{\dot{Z}_L}{Z_0}-1}{\dfrac{\dot{Z}_L}{Z_0}+1} \approx -\frac{\dot{V}_r}{\dot{V}_f} \quad \text{if } N \text{ is large} \qquad \text{Eq 18}$$

Note the minus sign. The SWR, a real number (not complex), is defined as:

$$\text{SWR} = \frac{1+|\dot{\Gamma}|}{1-|\dot{\Gamma}|} \approx \frac{1+\dfrac{|\dot{V}_r|}{|\dot{V}_f|}}{1-\dfrac{|\dot{V}_r|}{|\dot{V}_f|}} \qquad \text{Eq 19}$$

$$|\dot{\Gamma}| = \frac{\text{SWR}-1}{\text{SWR}+1} \approx \frac{|\dot{V}_r|}{|\dot{V}_f|}$$

The return loss, in dB, is defined as:

$$\text{RL (dB)} = -20\log|\dot{\Gamma}| = -20\log\frac{\text{SWR}-1}{\text{SWR}+1}$$

$$\approx -20\log\frac{|\dot{V}_r|}{|\dot{V}_f|} \qquad \text{Eq 20}$$

From this equation we see that RL increases rapidly as $\dot{V}_r$ approaches zero. Return loss, indicated by the $\dot{V}_r$ terminal of the directional coupler, is therefore a sensitive indicator that is widely used to fine-tune a network and optimize its impedance match over a frequency range.

SWR is the ratio of voltage (or current) at a physical location of maximum value to voltage (or current) at a physical location of minimum value along the length of a transmission line. For a lossless line, the value of SWR is the same everywhere along the line. Eq 19 tells us that for a given SWR the ratio of $|\dot{V}_r|$ to $|\dot{V}_f|$ is constant as the coupler is repositioned along the line. This ratio is also the return loss, so the return loss is also constant.

Also of considerable interest are the forward (incident) and backward (reflected) power waves. The concept of directed power waves is related to the Poynting vector of electromagnetics.[6] According to the theory, the conductors act as "guides" for the power flow, which is actually conveyed by the electric and magnetic fields within the dielectric medium. The power $\dot{P}_L$ in $\dot{Z}_L$ (assume for this discussion that R_L and X_L are in *parallel*) is a complex quantity. The real part is dissipated in R_L, and the imaginary part circulates between X_L and the power source. The real part, the "useful" power that is actually dissipated in the load resistance, is:

$$\text{Re}\left(\dot{P}_L\right) = P_{DISS} = \text{Re}\left(\frac{V_o^{\,2}}{\dot{Z}_L}\right) = \frac{V_o^{\,2}}{R_L} \approx \left.\frac{\left(N|\dot{V}_f|\right)^2}{Z_0}\right|_{\text{if SWR}=1.0} \qquad \text{Eq 21}$$

The forward real-power wave and the reflected real-power wave are given by:

$$P_F = \text{Re}\left(\dot{V}_o^{\,+}\,\dot{I}_o^{\,+}\right) = \text{Re}\left[\frac{V_o^{\,2}}{\dot{Z}_L\left(1-\dot{\Gamma}^2\right)}\right] = \text{Re}\left[\frac{V_o^{\,2}}{Z_0\left(1+\dot{\Gamma}\right)^2}\right]$$

$$\approx \frac{V_o^{\,2}/Z_0}{\text{Re}\left(1-\dfrac{\dot{V}_r}{\dot{V}_f}\right)^2}$$

$$P_R = \text{Re}\left(\dot{V}_o^{\,-}\,\dot{I}_o^{\,-}\right) = \text{Re}\left[\frac{V_o^{\,2}\,\dot{\Gamma}^2}{\dot{Z}_L\left(1-\dot{\Gamma}^2\right)}\right] \qquad \text{Eq 22}$$

$$= \text{Re}\left[\frac{V_o^{\,2}\,\dot{\Gamma}^2}{Z_0\left(1+\dot{\Gamma}\right)^2}\right] \approx \frac{V_o^{\,2}}{Z_0}\cdot\text{Re}\left[\frac{\left(-\dfrac{\dot{V}_r}{\dot{V}_f}\right)^2}{\left(1-\dfrac{\dot{V}_r}{\dot{V}_f}\right)^2}\right]$$

if N is large. The basic power relation is, as a comparison of Eqs 21 and 22 shows:

$$P_{DISS} = P_F - P_R \qquad \text{Eq 23}$$

In words, the total power dissipated in the load is equal to the forward real-power wave minus the reflected real-power wave. From Eq 22 we see how $\dot{V}_f$ and $\dot{V}_r$ are related to these waves. Finding the values of P_{DISS}, P_F and P_R requires a knowledge of V_o. For values of $N \geq 10$, V_o is almost identical to $|\dot{V}_{in}|$, and either value is sufficient in most applications. Also, a comparison of Eqs 20 and 22 shows that the ratio of reflected power to forward power in dB is equal to the return loss in dB times –1.

To measure P_F and P_R, Eq 22 requires measurement of V_o, $\dot{V}_f$ and $\dot{V}_r$. Eq 22 states clearly that the complex algebra involving $\dot{V}_f$ and $\dot{V}_r$ must be performed in exactly the manner indicated. This can be difficult in circuit design. A simpler approach that is widely used in power and SWR measurements is to use the relationship:

$$\mathrm{Re}\left(\dot{P}_F\right) = \frac{N^2}{Z_0} \cdot \dot{V}_f \cdot \dot{V}_f^* = \frac{N^2}{Z_0} \cdot \left|\dot{V}_f\right|^2$$

$$\mathrm{Re}\left(\dot{P}_R\right) = \frac{N^2}{Z_0} \cdot \dot{V}_r \cdot \dot{V}_r^* = \frac{N^2}{Z_0} \cdot \left|\dot{V}_r\right|^2 \qquad \text{Eq 24}$$

where * denotes complex conjugate, and from Eq 23:

$$P_{DISS} = \frac{N^2}{Z_0} \cdot \left[\left|\dot{V}_f\right|^2 - \left|\dot{V}_r\right|^2 \right]$$

In this equation the magnitude values are obtained by rectifying $\dot{V}_f$ and $\dot{V}_r$. We then perform the squaring and difference operations with dc log and antilog converter circuitry and op-amps. Note 1 describes this approach in detail. Digital signal processing would also be an excellent way to make these calculations. The same instrument could use $|\dot{V}_r|$ and $|\dot{V}_f|$ to get SWR, using Eq 19. For CW and SSB, a peak-power holding capacitor is added to the meter, using battery-powered op-amps or passive circuitry. One difficulty with this scheme is that for a given SWR, we cannot say whether $|\dot{Z}_L|$ is greater than Z_0 or less because the rectification process deletes the phase information that Eqs 17 and 22 require. Also, the diodes must have identical volt-amp curves, which is not very difficult to achieve. Several commercially available power/SWR meters with peak-holding have been reviewed in *QST*.[7]

At very low power levels, where diode rectification threshold problems and temperature-dependence become unmanageable, or whenever phase information is needed, a direct implementation of Eq 22 is necessary using high-frequency signal processing, although this is more difficult than processing rectified signals. Frequency translation to a low IF is employed (Note 5, Fig 16.10). At this low IF, DSP can use the methods of harmonic sampling (Note 5, chapter 7).

In the absence of such a special instrument to measure SWR, if a voltmeter is used to read $|\dot{V}_f|$ and $|\dot{V}_r|$, the meter can be set to full scale with $|\dot{V}_f|$ and then calibrated to convert $|\dot{V}_r|$ to SWR (Eq 19) or RL (Eq 20). If an accurate measure of the *true* load power P_{DISS} is wanted, we must first reduce $|\dot{V}_r|$ to almost zero (SWR ≈ 1.0) by some tuning procedure (Eq 22). Then $V_o \approx N|\dot{V}_f|$ and we get P_{DISS} from Eq 21. A common practice in Amateur Radio is that, if the SWR is less than 2.0, $|\dot{V}_f|$ is an "adequate" measure of true load power P_{DISS} within 0.5 dB, using the following calculation:

SWR = 2.0

$$\left|\dot{\Gamma}\right|^2 = \left(\frac{2-1}{2+1}\right)^2 = \frac{1}{9} = \frac{P_R}{P_F} = \frac{P_F - P_{DISS}}{P_F} \qquad \text{Eq 25}$$

Solve for P_{DISS}:

$$P_{DISS} = P_F\left(1 - \left|\dot{\Gamma}\right|^2\right) = P_F \cdot \frac{8}{9} \quad \rightarrow \quad -0.51\ \mathrm{dB}$$

The error is on the conservative side, which helps satisfy the legal power issue (from Eq 23, $P_F \geq P_{DISS}$). If a transmatch is used at the station, we usually tune it for SWR ≈ 1.0 anyway, which accomplishes the desired calibration.

Directional couplers with rectifiers are widely used in solid-state power amplifiers as ALC (automatic level control) detectors and to protect against transistor burnout.[8]

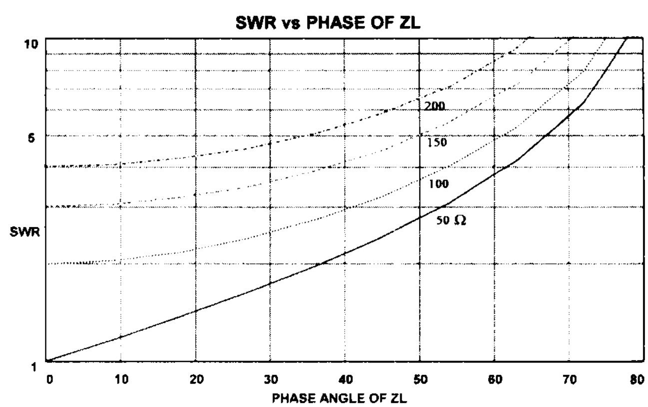

Fig 4— SWR for four values of complex load for phase angles from 0 to 80 degrees.

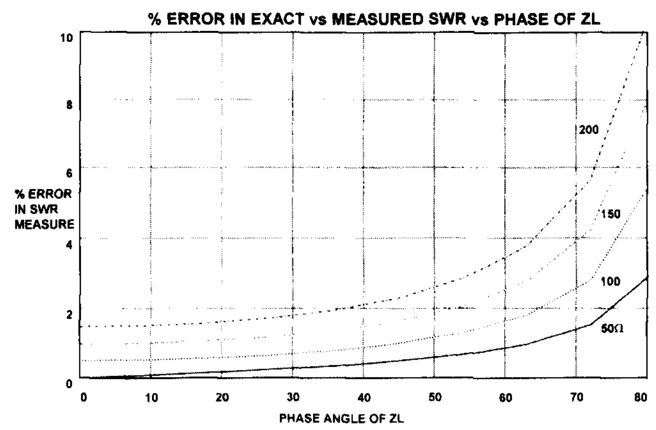

Fig 5—Comparison of the exact value of SWR versus approximate value in Fig 4.

Finally, a bit of perspective regarding forward power and reflected power. In the classical *lumped-circuit* point of view, if a generator with output resistance Z_0 "sees" a load not equal to Z_0, a mismatch loss occurs, meaning that the maximum available power is not transferred from the generator to the load. In the *directed power wave* point of view, we say that the forward wave is what the generator "tries" to send to the load. The mismatch loss is the fraction of available power that is not accepted by the load but is returned (reflected) from the load back to the source. The difference between forward and reflected power is equal to the power that is actually accepted by the load. It is also equal to the power that is actually *delivered* by the generator. These two different points of view are numerically identical; they are two different ways of saying the same thing.

Performance with a complex load

The above equations involve some very nasty complex algebra calculations. The personal computer program *Mathcad 5.0* removes all of the pain and gives answers almost instantly.[9] Printouts of the *Mathcad* problem worksheets and the derivations of all the previous equations are available from ARRL and will not be presented here.[10] Instead we will discuss the results for the general case of a complex load. The values of $\dot{V}_f$ and $\dot{V}_r$ will be related to the quantities mentioned in the previous sections. To limit the scope of this article, we will look at just two items.

One is the exact values of SWR for a complex load for four values of $|\dot{Z}_L|$ at phase angles from 0º to 80º. These are shown in Fig 4. Beyond 80º, the SWR becomes extremely large. It is interesting to see how SWR depends on the phase angle of $\dot{Z}_L$. For instance the SWR=4.0 line could represent 200 Ω at 0°, or 50 Ω at 62°, and so forth. Fig 5 compares these exact SWR values, calculated using Eq 19, to the approximate value in the same equation for $N = 10$. The exact value of $\dot{\Gamma}$ used to get SWR is obtained from Eq 18. The fractional error in the approximate SWR is very small until the phase angle becomes large.

The second item compares the actual and approximate values of four values of $\dot{Z}_L$ at phase angles from 0º to 80º using the approximations of Eqs 8 and 10. Fig 6 is the

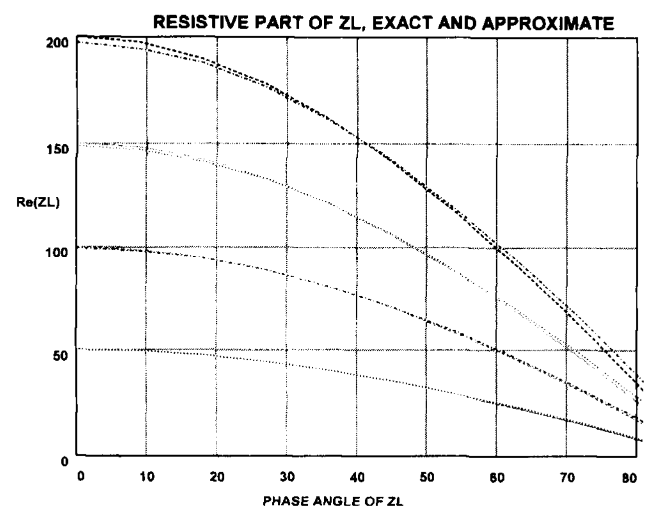

Fig 6—The resistive part of exact and approximate values of Z_L.

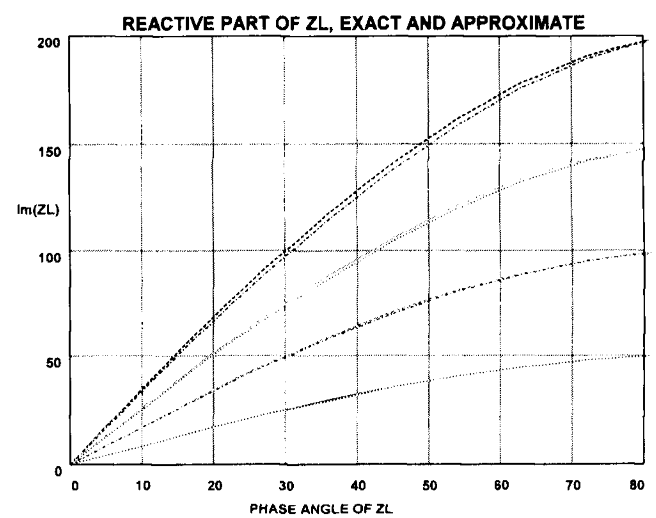

Fig 7—The reactive part of exact and approximate values of Z_L.

resistive part and Fig 7 is the reactive part of the calculated $\dot{Z}_L$.

These four plots show the best that can be done, based on measurements of $\dot{V}_f$ and $\dot{V}_r$, without computer processing. Actual hardware would try to achieve these results.

Simulations

Simulation is a better tool than math with which to investigate the coupler in more detail, including imperfections in T1 and T2 and stray L and C and time delays in various places. Using a circuit analysis program, changes can be introduced easily and in controlled quantities. In particular, the two transformers can alter coupler performance, especially over a wide frequency range, if they are less than ideal. We will use the new *ARRL Radio Designer* (*ARD*) program for the analysis;[11] the various SPICE programs work well also. Because of space limits, we can only introduce this subject, but with the software, countless variations are possible and easy to check out.

Fig 8 is the diagram of the circuit that is implemented by the very simple *ARD* netlist of Fig 9. I use *ARD*'s voltage probe feature to look at terminals V_{in}, V_{out}, V_f and V_r. (Only the voltage magnitudes are used in this example). This one-port network is driven by a 1.0-V generator with a 50–Ω source (default) resistance. The resistor from the V_{out} terminal to ground (200 Ω in this example) can be replaced by various R, L and C combinations or transmission lines. A slightly more advanced listing would use the coupler as a two-port subcircuit in a higher-level *main* system. To use this approach, the *hierarchy* requirements of ARD must be met properly. The frequency sweep is exponential from 1 to 100 MHz.

Fig 10 is a plot of the four voltages. This plot illustrates the effects of two major imperfections, showing how an accumulation of things can affect the coupler. The 18-µH toroids (two T80-2 cores with 40 turns of #24 wire, having a Q of 250 at 2.5 MHz) were found by measurement to be parallel self-resonant at about 20 MHz, so I placed a 3.5-pF capacitor across each coil for the simulation. Minor series and parallel resonance effects were found in the 90 to 105 MHz region, but these were not simulated. The turns ratio N for this simulation is 10 (inductance ratio 100:1). The coefficient of coupling K was reduced to 0.85 as a bad example. The plots show the following:

- The inductance of the coils is marginal at 1.8 MHz. V_{in} and V_{out} (left-hand scale) show a roll-off. V_f and V_r (right-hand scale) are also affected. The coils are very good at 30 MHz and beyond.
- The small value of K, in combination with the values of inductance and self-capacitance of the coils, affects the high frequency response. The increasing imped-

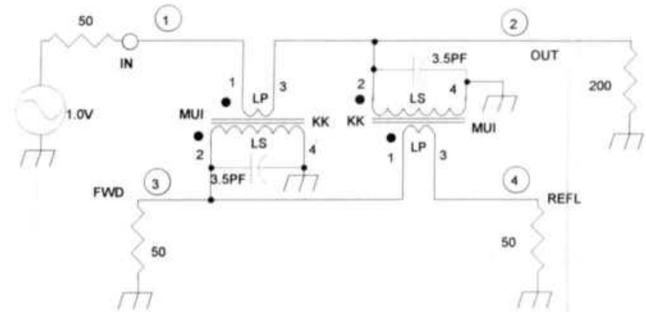

Fig 8—Diagram of the circuit used for *ARRL Radio Designer* simulation.

```
Compact Software - ARRL Radio Designer 1.0  23-JAN-95  02:57:29
File: a:\dircplr.ckt

*DIRECTIONAL COUPLER

LP:1.8E-7
LS:1.8E-5
KK:0.85

BLK
   MUI 1 3 2 0 L1=LP L2=LS K=KK
   MUI 3 2 4 0 L1=LP L2=LS K=KK
   CAP 2 0 C=3.5PF
   RES 3 0 R=50
   CAP 3 0 C=3.5PF
   RES 4 0 R=50
   RES 2 0 R=200
CPLR: 1POR 1
END

FREQ
  ESTP 1MHz 100MHz 100
END
```

Fig 9—The *ARRL Radio Designer* netlist used to simulate the circuit of Fig 8.

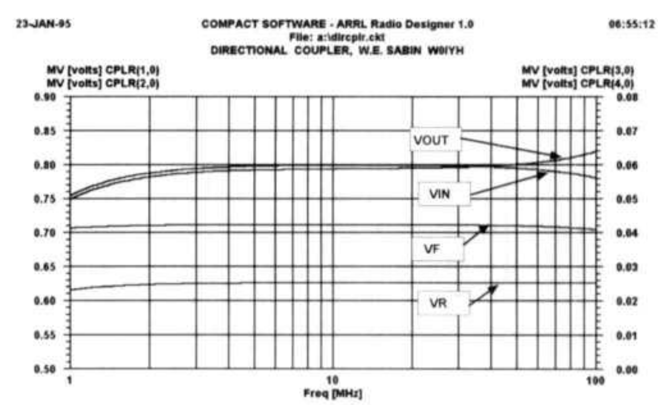

Fig 10—Plot of *ARRL Radio Designer* simulation results from 1 to 100 MHz.

ance of the transformer windings causes V_{in}, V_{out}, V_f and V_r to change. Also, $|\dot{V}_r|$ and $|\dot{V}_f|$ are both smaller than they should be (at all frequencies). But interestingly, because both transformers are equally affected, the *ratio* of $|\dot{V}_r|$ to $|\dot{V}_f|$ is only very slightly affected by the value of K, at least in the flat-frequency-response range. This ratio is the one that is most used in SWR and power measurements. The simulator shows that higher values of K improve the high-frequency response, improve the values of V_f and V_r considerably, and greatly reduce the influence of the 3.5-pF capacitors, so tight coupling in the transformers is an important item. It turns out that this tight coupling is not hard to get.

Some other things worth looking at would be the following:

- Phase shifts between the four terminals. These can vary according to the kind of load impedance connected to the OUTPUT terminal. This would be very important in many applications. Amplitude frequency response changes suggest nonlinear phase changes also.
- Effects of the inductances of transformer lead lengths.
- Microstrip from the transformers to the four terminals.
- Capacitance from primary to secondary, to ground and to the case.
- The simulator can find the four-port S-parameters under all of the conditions mentioned above.
- Stray effects or diode problems that might make the SWR readings change with power level. This is a frequently encountered complaint (see Note 7).

The best way to evaluate K is to measure the voltages at the four ports with an accurate RF voltmeter (a Boonton 92-A, in my case), to see if they match those predicted by Eq 13. I found that with a 40-turn toroid and RG-213 coax (with Faraday shield) through the toroid hole (that is, 1 turn) the value of $|\dot{V}_f|$ in the flat-response region was within 0.2 dB of the predicted value. This means that K is at least 0.98, as found by to the simulator.

Conclusion

This brief presentation may serve as a guide to a better understanding of the directional coupler. Like many "simple" contraptions, it is not really all that simple. One of its big advantages is that with careful design it can be used to make all kinds of complex impedance and transmission-line measurements at high transmitting power levels or at low receiving levels and can be a permanent part of the equipment. And it can serve a number of other useful functions, as I have suggested.

Notes

[1]Grebenkamper, J. KI6WX, "The Tandem Match," QST, Jan 1987. See also "Technical Correspondence," July, 1993. See also the 1995 edition of *The ARRL Handbook*, chapter 22, and *The ARRL Antenna Book*, 17th edition.

[2]McDonald, R.S., WB7CLV, "Low Cost, Wideband Dual Directional Coupler," *RF Design*, May/June 1982.

[3]Lewallen, R., W7EL, "A Simple and Accurate QRP Directional Wattmeter," *QST*, February 1990. See also *The ARRL Handbook*, 1995 edition.

[4]Spaulding, W., "A Broadband Two-Port S-Parameter Test Set," *Hewlett-Packard Journal*, Nov. 1984.

[5]Sabin, W.E., WØIYH, Schoenike, E.O. and others, *Single-Sideband Systems and Circuits*, chapters 12, 13 and 16, McGraw-Hill, New York, 1987 (also 2nd edition, 1995).

[6]Kraus, J.D., W8JK, *Electromagnetics*, 4th edition, McGraw-Hill, New York, 1992.

[7]Healy, Rus, NJ2L, "*QST* Compares:Peak-Reading MF/HF Wattmeters," *QST*, February 1991, p 33.

[8]Blocksome, R., KØDAS, "50-W Amplifier Project," *The ARRL Handbook*, 1995 edition, p 17.93. See also the transceiver discussion in the main text of chapter 17.

[9]MathSoft, Inc., 101 Main St, Cambridge, MA 02142.

[10]For a printout of the equation derivations and the *Mathcad* worksheet, send a self-addressed, stamped envelope to: Technical Department, ARRL, 225 Main Street, Newington, CT 06111. Specify that you want the March 1995 QEX template (Sabin).

[11]Newkirk, D., WJ1Z, "Introducing ARRL Radio Designer," *QST*, October, 1994, p 21.

A Modular, High-Performance 5.76-GHz Transverter

Building a transverter for 5.76 GHz is easier than ever.

By Rus Healy, NJ2L

Improvements in printed filter technology, monolithic 50-Ω gain blocks and hotter GaAs FETs have substantially decreased the cost and difficulty of getting on the amateur microwave bands in recent years. But equipping your station for 5.76 GHz still presents a significant challenge. The key pieces to build a high-performance system—without any surplus stuff—are all available, but you have to find those pieces and glue things together. Of course, you can build KK7B's simple bilateral mixer transverter for 5760, which is available from Down East Microwave,[1] but it puts out very little power and requires complex switching to use in a system optimized for weak-signal operation. Using existing pieces and some fairly new parts, I've developed a simple but solid-performing 5.76-GHz transverter that's quite easy to duplicate. This is not a cookbook project, but gives the sources for all the necessary blocks in such a transverter and references for articles that describe the fabrication of the home-brew parts.

[1]Notes appear on page 15.

111 Woodridge Crossing
Henrietta NY 14467-8923
Internet: rhealy@mcimail.com

Overview

This transverter uses the block diagrams in Fig 1. My local oscillator is a surplus dielectric resonance oscillator (DRO) that isn't readily available, but other LO options exist. I use a dual mixer with integrated image-stripping filters. This mixer, designed by Paul Wade, N1BWT, and available from Down East Microwave, is the most compact, inexpensive and easily reproducible version I've seen for this band. The filtering on this mixer board is adequate for any IF of 144 MHz or higher. I use a 432-MHz IF in my system because my LO runs at 6192.2 MHz (5760.1 + 432.1 = 6192.2). The mixer board's filters are the only elements in the system that require tuning. This is easily done with the right test equipment, but a Down East Microwave 1152-MHz weak-signal source also provides the necessary alignment signal.

The transmitter chain is dirt simple, using a single Hewlett-Packard GaAs MMIC following the mixer for about 3 mW output. In the receive chain, I cascaded a two-stage GaAsFET preamplifier with another GaAs MMIC ahead of the mixer, and a MAR-6 post-mixer amplifier. I included the post-mixer stage to increase the transverter's conversion gain before I added the GaAsFET preamp. I left the MAR-6 stage in place after I added the preamp, at which time I also added the 20-dB attenuator at the IF output. The post-mixer amplifier/attenuator combination protects the receive mixer from inadvert-

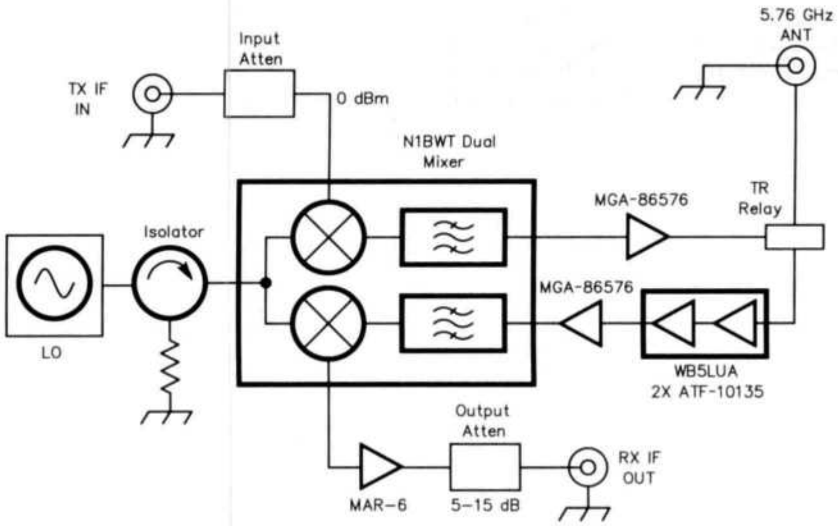

Fig 1—Block diagram of the 5.76-GHz transverter.

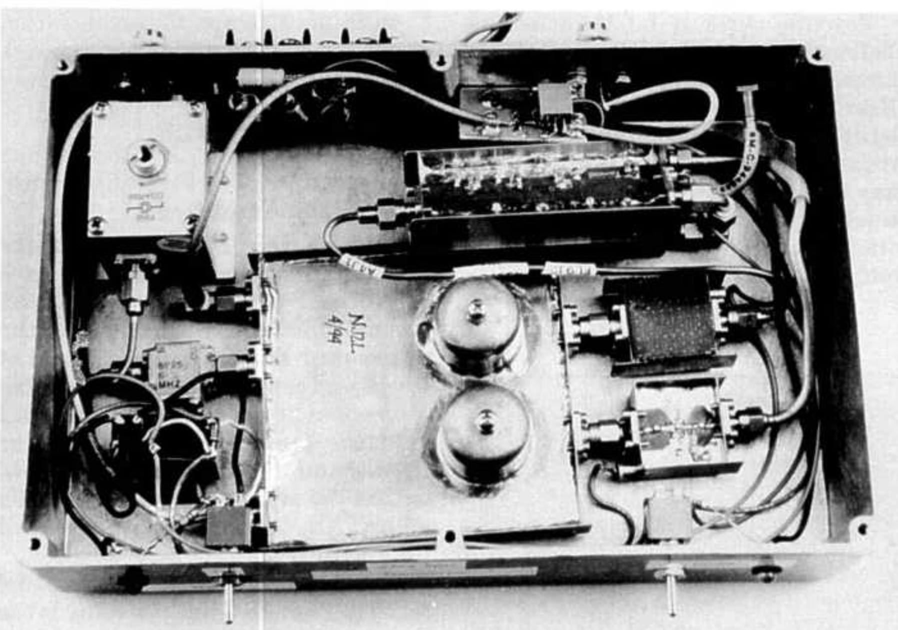

Fig 2—An inside look at the 5.76-GHz transverter. The chassis dimensions are 2 x 8.5 x 5.75 inches. This enclosure is usable only with a physically small local oscillator (like the DRO in the upper left), or with an external LO.

Table 1—Measured Transverter Performance

Receive Converter Noise Figure: 1.6 dB.
Receive Conversion Gain: 30 dB (variable—see text).
Transmitter Output at 1 dB compression: +3 dBm.
Intermediate Frequency: 432 MHz.*
Supply Voltage: +10.5 to +16 V.
Current Drain: receive, 75 mA; transmit, 110 mA.
*144 MHz or a higher IF is possible with the appropriate LO.

ent application of transmit drive and a subsequent smoke release from the mixer diodes. (During the second contest in which I used this system on the air, the post-mixer amplifier did its job and saved the mixer from me!)

The transverter is built in a 2 × 8.5 × 5.75-inch die-cast aluminum box. Since only the T-R relay driver requires more than 10 V dc, I power all the internal circuitry except that driver from a 10-V, low-dropout regulator (a Linear Technologies L4810). This regulator has rather limited current capability (0.4 A), but requires only 0.4 V of overhead to maintain regulation. If you operate from batteries, I recommend using a low-dropout regulator to power the transverter's circuits. The National LM2941T is a good choice, as it can source more current than the L4810 and is adjustable.

Each internal assembly is terminated by female SMA connectors. Interconnections are made with UT-141 and UT-085 semirigid coax. Fig 2 shows the complete transverter. Details of each stage follow.

Local Oscillator

As mentioned earlier, I used a DRO as the LO source in my transverter. Other options include surplus phase-locked "brick" sources, which are inexpensive and relatively common in the 5 to 7-GHz range at flea markets, and Zack (KH6CP) Lau's 5616-MHz homebrew LO described in May 1993 *QEX*.[2] The mixer needs between +5 and +13 dBm of LO energy, so any clean, stable source in this range will do the job. The DRO is very small, runs on +10 V at only 35 mA, puts out +10 dBm, and is very clean. But it drifts—a *lot*. It's not unusual for the thing to drift several kilohertz per minute until it's been powered up for a couple of hours, and it doesn't always wind up on the same frequency. Its total drift range is more than 100 kHz, so it takes some hunting to find stations! To compensate for the drift, I use the harmonic from a Down East Microwave weak-signal source running at 1152.031 MHz to find my conversion frequency during operation on this band. An isolator between the LO and the mixer board helps stability by giving the LO a constant load, and it's a good idea to use an isolator no matter what kind of LO you have. If your LO puts out significantly more power than your mixer needs, a 50-Ω attenuator between the LO and mixer board will serve the same purpose.

Brick LOs are much more stable than my DRO, usually staying within a few hundred hertz over long periods of time, but they typically draw hundreds of milliamps from –18 to –24 V power supplies. I think the best solution is KH6CP's 5616-MHz LO. It's a bit time-consuming to build (it uses three PC boards, one of which is available from Down East Microwave), but it runs on low dc voltage and doesn't draw as much current as the phase-locked bricks. Based on my experience with a 10.8-GHz LO built using the same techniques, a carefully built version of Zack's 5616-MHz LO should be nearly as stable as the brick variety. (After a few minutes of warm-up, my 10.8-GHz LO drifts less than 1 kHz over time and moderate temperature variations.)

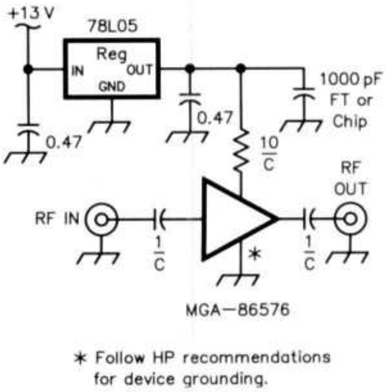

Fig 3—MGA-86576 5.76-GHz amplifier stage used in the transmit and receive paths. All capacitors are chips; those in the RF path are ATC or other high-quality 50-mil ceramic chips. For best performance, avoid using cheap chip capacitors in the RF path at these frequencies.

GaAs MMIC Amplifier Stages

A year or so ago, HP announced the MGA-86576 GaAs MMIC, which has usable gain to at least 12 GHz. It's optimized for the 1.5 to 8-GHz range, has lots of gain and a low noise figure, and is easy to use, requiring only a 5-V supply. It seemed the ideal part to use in both the transmit and receive legs of my transverter. The part costs around $14 in small quantities.[3] HP specifies this device's nominal 5.7-GHz performance as an impressive 19 dB gain and 2.3 dB noise figure.

Starting with a 0.031-inch-thick Teflon PC board originally intended to house three silicon MMICs (Down East Microwave part number UA-3), I built the two MMIC amplifiers for my transverter. Of course, you can use any 50-Ω microstrip PC board that's no thicker than 0.031 inch for these stages, but the UA-3 is ready-made and, when cut in half, easily makes two amplifiers. See the schematic in Fig 3 and photo in Fig 4. In building these stages, I used information in the HP data sheet for the MGA-86576, being especially careful to give the MMIC ground leads the shortest path to the PC board ground. At these frequencies, all kinds of bad things happen if the ground leads are too long. The HP data sheet recommends a minimum of two through-board grounds, as close as possible to each of the device's ground leads. I used four wires at each ground lead, as close as possible to the device body.

The amplifiers, like all the other 5.76-GHz circuits in the transverter, are packaged with brass-strip walls using the technique I described in an earlier *QEX* article.[4] The first amplifier I built has only about 12 dB gain and a 3-dB noise figure at 5.7 GHz. So I used it as the transmit amplifier. The second one is closer to what I expected: 15 dB gain and a 2.5-dB noise figure. This one is the receive-side amplifier. I made no attempt to tweak either stage for better performance, even though the HP data sheet shows that this device's matched noise figure at 6 GHz is around 1.6 dB.

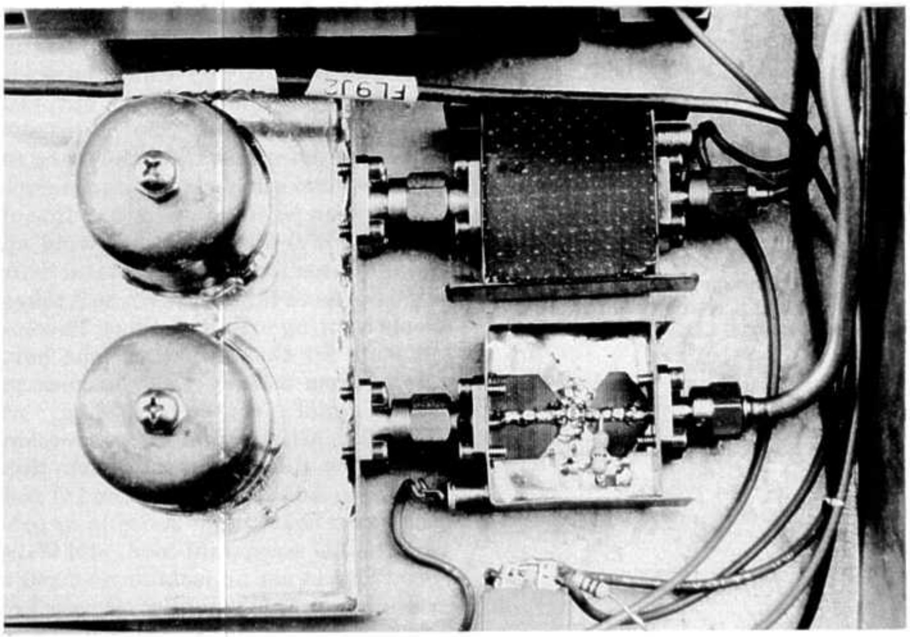

Fig 4—This photo shows the simplicity of the MGA-86576 amplifier. A 5-V regulator and associated low-frequency bypassing are located on the opposite side of the PC board. Note the microwave absorbing material in the top of the receive-side (upper) amplifier.

Preamplifier, T-R Switching and Post-Mixer Amplifier

Between the T-R relay and the MMIC receive amplifier stage is a WB5LUA two-stage, ATF-10135 preamplifier. With this setup, the transverter has a net noise figure of 1.6 dB and conversion gain adjustable from about 20 dB to well over 35 dB. I built the pre-amplifier's active bias circuitry on the back side of the board so that the preamp can be fed directly with a 13.8-V source—a trick I learned from KH6CP.

The T-R relay is an SPDT model rated to 12 or 18 GHz. The relay is the one component in the transverter that's best to buy surplus. This one I got at Dayton for around $25, whereas new relays in this class cost well over $200 each. They're plentiful at VHF/UHF conference flea markets and all the larger ham gatherings. Since this relay has a 28-V coil, I built a small circuit using an ICL-7660 IC to develop the relay voltage from 13.8 V.[5]

On the IF side of the receive mixer, it's a good idea to include a rugged gain block to prevent inadvertent mixer damage, as discussed earlier. It also helps the transverter overcome inadequate conversion gain or compensate for a deaf IF radio. To provide this function, I built an MAR-6 amplifier on a piece of unetched copper-clad G-10 PC board material a couple of inches square. A solder lug on one of the receive IF output connector's mounting screws supports the board. Between the MMIC output and the connector center pin is a 20-dB pi-network resistive attenuator, which cancels most of the MMIC's gain. A variable attenuator can be useful here to tweak the transverter's conversion gain; use a 1-kΩ pot in the series leg and two 220-Ω shunt resistors.

In the transmit path, the mixer board includes a gap in the IF microstripline so that you can put an input attenuator on the board. Mine uses a 15-dB pad to knock down the 432-MHz drive level from my IF radio to the appropriate level for the mixer. Keep the IF drive at the mixer diode below +3 dBm.

Squirrels

As can be expected inside any box that has more than 30 dB of gain at the desired frequency (and probably more gain at other frequencies), oscillations can occur if you're not lucky. I wasn't. The trouble came when I installed the preamplifier in the transverter. Noise figure readings became unstable and several dB higher than they should have been, and a strong signal occasionally swept across the desired receive frequency. To fix the problem, I made several changes. First, I had built the ATF-10135 preamplifier with 110-mil ATC chip capacitors, rather than the recommended 50-mil caps, because that's what I had on hand. I replaced them with the correct capacitors, which made a big difference. My noise figure still changed by more than 1 dB, depending on whether the cover was on the transverter, so I kept looking. I removed the final coupling capacitor from the preamp to cut its radiation as much as possible. (The dc path between the two amplifiers is blocked by a capacitor in the input line of the MGA-86576 amplifier.) This change also helped. To see whether the MGA stage was oscillating, I replaced the output coupling capacitor with a 15-Ω chip resistor. This made no difference, so I left it alone. The final fix was to add a piece of surplus microwave-absorbing material in the top of the MGA-86576 stage.

The receive converter is now stable and shows the same gain and noise figure with the top cover on or off. If you want to avoid the same kind of stability fight I had, which is particularly important if you don't have access to a noise-figure meter, you may want to omit the MGA-86576 amplifier stage in the receive converter. The best achievable noise figure will be somewhat more than 2 dB for the entire transverter, but a 2-dB noise figure is better than an oscillating receive chain! Of course, the key construction goal is to properly package each stage for best isolation, but this is tricky to do when the stage's enclosure forms a waveguide above cutoff.

Summary

This transverter works pleasingly well. I've worked several stations at 50-mile-plus distances during the last two ARRL VHF contests, using this transverter driving a surplus 15-W TWTA. My 5.7 GHz antenna is a 24-inch aluminum dish with a WA3RMX triband feed. The system performance is good enough that I expect it to be capable of making 200-mile QSOs under flat conditions with a similar station at the other end. Although finding a 15-W TWTA or other high-power amplifier is likely to be difficult, one easy way to get 50 to 75 mW output from the transverter is to use a second WB5LUA preamplifier, fed directly by the mixer, in lieu of the MGA-86576 transmit stage. In the 1989 *QST* article in which Al Ward described these preamplifiers, he mentions bias conditions for the ATF-10135 that are more appropriate for power amplifier use.[6] With this kind of power output into a 24-inch or larger dish, you'll be pleasantly surprised at what you can work. For a better signal with non-surplus components, you need to break out your wallet for power GaAsFETs or IMFETs.

Here in western New York, and all over the northeastern US, enough stations are active on the 5.7-GHz band to make this transverter really worthwhile to take along on contest efforts. The transverter is easy and cheap enough to build that even if there's not much activity on this band in your area, it's feasible to build two of them and pass one around to other interested hams so you have someone to work—and you can both experience the fun of making microwave QSOs!

Notes

[1]Down East Microwave, Inc, 954 Rte 519, Frenchtown, NJ 08825, tel: 908-996-3584, fax: 908-996-3702. Catalog available.
[2]Lau, Z., KH6CP, "A 5616-MHz Local Oscillator," *QEX*, May 1993, pp 15-19.
[3]See Note 1.
[4]Healy, R., NJ2L, "Building Enclosures for Microwave Circuits," *QEX*, June 1994, pp 15-17.
[5]Fogle, R., WA5TNY, "+12 to +24 V Switching Power Supply," *Proceedings of Microwave Update '91*, pp 332-333.
[6]Ward, A., WB5LUA, "Simple Low-Noise Microwave Preamplifiers," *QST*, May 1989, pp 31-36, 75.

Measuring 9600-Baud Radio BER Performance

DSP techniques make testing a G3RUH-compatible radio easy.

By Jon Bloom, KE3Z

One of the jobs of the ARRL Lab is to test the performance of equipment sold to amateurs. With the new crop of 9600-baud radios coming out, we had to develop a technique for testing their performance. The best way to test the performance of a radio used for digital communication is, by far, to test the bit-error rate (BER) that the radio provides under various conditions. BER is a conceptually simple metric that answers the question: How many of the bits get through correctly when a data stream is passed through the system?

The system we developed uses a Texas Instruments DSP Starter Kit (DSK) board that includes a TMS320C26 processor. Figs 1 and 2 show the circuitry of the BER test box built in the ARRL Lab. The DSP generates a test signal that is passed through the system under test. For receiver testing, the signal modulates a low-noise FM signal generator that feeds the radio being tested. The demodulated output of the radio goes to the DSP input so that the demodulated signal can be compared to the transmitted signal. To test transmitters, the DSP output test signal is applied to the modulation input of the transmitter under test. The transmitter RF output is attenuated to a low level, then applied to the Lab-built test box where it is mixed with an unmodulated signal from a signal generator. The resulting IF signal is demodulated by a low-distortion demodulator, and the demodulated signal is routed to the DSP input for comparison with the generated signal.

225 Main Street
Newington, CT 06111
email: jbloom@arrl.org

G3RUH Signals

The 9600-baud system used for amateur packet radio, both terrestrially and via the UoSat packet satellites, uses signals handled by the G3RUH modem design. In this system, the binary data stream coming out of a TNC is first "scrambled" to remove any dc component of the signal. Scrambling, which has nothing to do with encryption or data hiding, is simply encoding that ensures that, on average, there are as many 1-bits in the data stream as there are 0-bits. The average voltage of the data signal is thus constant. The scrambled data signal is then used to generate shaped pulses. The shaped-pulse signal is what is applied to the modulation input of the FM transmitter.

On reception, the shaped-pulse

signal is filtered and limited, to recover the scrambled data stream. A clock-recovery circuit generates a clock signal that is synchronous with the incoming data. Using this clock, the modem descrambles the data stream, with the end result being a binary data signal identical to the transmitted data signal.

Since our test system has to generate and receive signals like those of the G3RUH modem, some discussion of the pulse shaping used is necessary. The general problem to be solved when sending digital data using FSK is to limit the bandwidth of the baseband (data) signal before applying it to the modulator. But you have to be careful how you do that.

When we limit the bandwidth of a pulsed signal, we necessarily stretch the pulses in time. That is, a signal that is bandlimited cannot also be time limited. That means that in limiting the bandwidth, we cause each pulse to overlap adjacent pulses. In theory, each pulse overlaps *all* of the other pulses, but as you go further away in time from a particular pulse, its amplitude gets smaller and smaller.

So, we need to find some way of allowing the pulses to overlap their neighbors without interference. One approach to doing so is to shape the

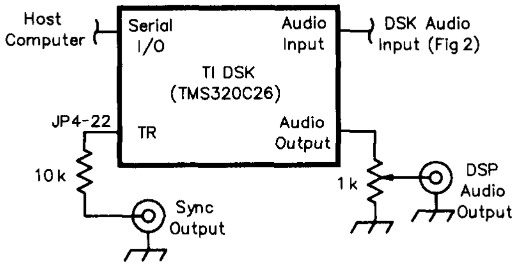

Fig 1—Diagram of the BER test connections to the TI DSK.

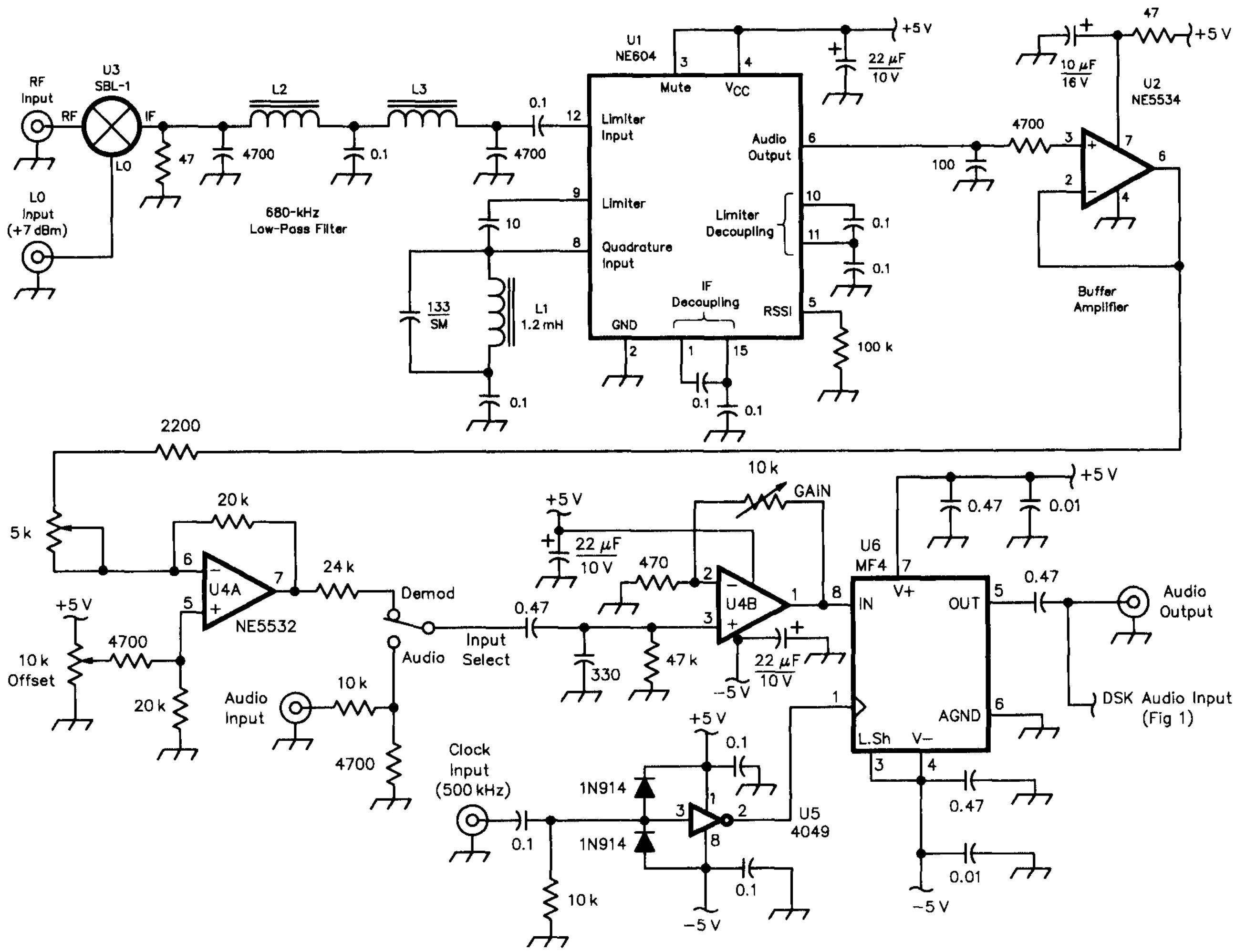

Fig 2—Schematic diagram of the BER test box circuit.

L1—1.2-mH Toko 10RB fixed inductor. (Digi-Key part TK4401-ND.)

L2, L3—41 turns #28 enam wire on a T-50-1 toroid core.

pulses so that, while each pulse does overlap its neighbors, the amplitude of that pulse is zero at the center of each of the other pulses. That way, we can sample the signal at the center of each pulse period and see only the signal from the current pulse; none of the other pulses contributes any amplitude to the signal at that time.

The spectrum of one pulse that has these characteristics is straightforward. It is flat from 0 Hz out to some chosen frequency, then rolls off with a cosine-shaped curve, reaching –6 dB at one-half the baud rate.[1] It continues rolling off with this cosine curve until it reaches zero. In the G3RUH system, the spectrum begins rolling off at 2400 Hz, reaches the –6-dB point at 4800 Hz and reaches zero at 7200 Hz.

In the time domain, the pulse shape that results from such a spectrum has a maximum at the center of the bit period, then decreases in amplitude as we move away from the center of the bit. The pulse signal goes negative, passing through zero at the center of the preceding and following bits. As we go farther away in time from the bit center, the signal alternates between positive and negative values, always passing through zero at the center of each bit. There are other spectra that have pulse shapes that reach zero at the center of all the other pulses, but the benefit of the raised-cosine spectrum is that the pulse amplitude falls off rapidly with time. This is important because any amplitude or phase distortion present in the system is likely to cause the zero-crossing points of the pulse to shift in time, causing ISI. Since the amplitude of the pulse is small near the center of other pulses, the potential for harmful ISI is also small.

Since each bit of the shaped-pulse signal now extends across multiple bit periods—both preceding and following bits periods—we must take this into account in generating our signal. And, since this is DSP, what we are generating is a *sampled* version of the signal. What we must end up with at any sample is a signal that comprises a component from the current bit, preceding bits and following bits. Theoretically, we need components from *all* of the bits in the data stream, but the amplitude of each pulse falls off so rapidly that only a few successive bits need be used to generate any given sample. In this system, we chose to include components of the current bit and the four preceding and four following bits.

Note that only 1-bits contribute to the signal; 0-bits generate no pulse. If we were to send a continuous stream of 0-bits, we'd get no pulses at all. (Of course, the scrambler circuit ensures that will never occur in a real transmitted data stream.) So, for each sample we need to add up the contribution of the current bit and the contributions of eight other bits, some of which may be 0-bits that make no con-

[1]Notes appear on page 23.

User-Defined Parameters:

Sampling rate: $f_s := 38400$ Baud rate: $R := 9600$ # bits: $b := 9$

System bandwidth: $B := 7200$

Calculated parameters:

$f_o := \frac{R}{2}$ $f_1 := 2\cdot f_o - B$ $n := \frac{f_s}{R}\cdot b$ $n = 36$

$f_\Delta := B - f_o$

$$h_e(t) := \left(\frac{\sin(2\cdot\pi\cdot f_o\cdot t)}{2\cdot\pi\cdot f_o\cdot t}\right)\cdot\left[\frac{\cos(2\cdot\pi\cdot f_\Delta\cdot t)}{1-(4\cdot f_\Delta\cdot t)^2}\right]$$ Impulse response function

$t_d := \frac{1}{f_s}$ Sampling period

$i := 0,1..n-1$ $t_i := \left(i - \frac{n-1}{2}\right)\cdot t_d$ Time values

$h_i := h_e(t_i)$ Impulse response of filter

$scale := \frac{2}{(\max(h) - \min(h))}$ $scale = 1.81101$

$a_i := |h_i|$ $s_i := \frac{h_i\cdot scale}{\sum a}$ Normalization of filter coefficients $j := 0,1..\mathrm{floor}\left(\frac{n-1}{2}\right)$

WRITEPRN(IMPULSE) $:= s_i$

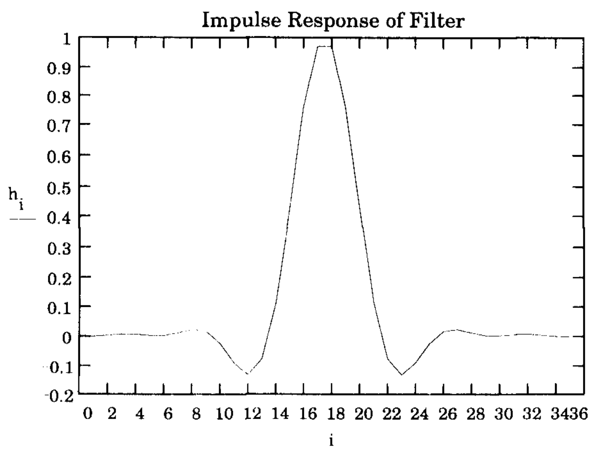

s_j
-0.001
$-6.1271\cdot 10^{-4}$
$7.4531\cdot 10^{4}$
0.0019
0.0016
$2.9393\cdot 10^{-4}$
$3.8545\cdot 10^{-4}$
0.0036
0.0075
0.0054
-0.0086
-0.0311
-0.0452
-0.0269
0.0393
0.1453
0.2571
0.329

Fig 3—This *Mathcad* worksheet calculates the impulse response of the FIR filter used to generate the shaped-pulse signal.

tribution. The contribution of a particular preceding or following 1-bit is the amplitude of its pulse at the present time. To keep things simple, we use a sampling rate that is a multiple of the baud rate—and thus a multiple of the pulse rate.

The method used to implement this pulse forming is an FIR filter. The impulse response of the filter is simply the samples that comprise a single shaped pulse, extending over nine bit periods. Our sampling rate is four times the bit rate, so the impulse response is 4×9=36 samples long. A *Mathcad 5.0* worksheet, shown in Fig 3, calculates the impulse response.

If we feed a single sample of amplitude 1 into the filter, preceded and followed by 0-amplitude samples, the resulting output will be a single copy of our shaped pulse, as shown in the *Mathcad* graph in Fig 3. To generate our data stream, we input the present data value (1 or 0) at one sample, follow it with three samples of 0, then input the next data value. At any time, the FIR filter contains zeroes in all except (possibly) 9 locations, representing the 9 successive data bits. The output of the filter at any sample time comprises components of 9 data pulses, which is what we want for our shaped-pulse signal.

Now that we know how to generate the shaped-pulse signal from a data stream, we need to think about how to generate the data stream itself. We want to generate a data stream that mimics the scrambled signal of the G3RUH modem. The scrambler in the modem is a tapped shift register with feedback. The logic equation for this circuit is:

$$y = x_0 \oplus x_{12} \oplus x_{17}$$

where y is the output of the scrambler, x_0 is the current input bit, x_{12} is the 12th previous input bit and x_{17} is the 17th previous input bit. Generating the test data stream is done by making x_0 always a 1, implementing a shift register in software, and calculating y for each new data bit—once every four samples. Note that this is essentially the same signal generated by the G3RUH modem in its BER test mode.

Counting Bit Errors

Having generated a test signal, we now need to consider how to compare the signal coming back from the system under test to the signal we transmitted. In passing through the tested system, the signal will be delayed by some amount, and the amount of delay will vary from one system to another. What we need to do is determine what the system delay is, then remember what our transmitted signal was that far back in the past in order to compare it to the samples of the received signal. But we are only interested in the value of the received signal at one time during each bit period: the center of the bit.

The DSP software handles this need using a two-step delay process. First, the operator will tell the DSP system how many samples of delay there are between the transmitted and received signals. Of course, the system delay is not likely to be kind enough to let the center of the received bits fall right onto one of our samples—there are only four samples per bit, after all. So, the second step is to adjust the phase of the DSP's transmit and receive sample clocks. The combination of these two techniques lets us adjust the DSP's delay with fine resolution.

This calibration procedure is performed using a dual-channel oscilloscope. One channel is connected to the *sync* signal from the DSK, the other channel is used to display the demodulated signal that is being fed into the DSK input. The operator first commands the DSK to generate a calibration signal. The DSK does so by passing a single 1-bit through the FIR filter described previously, followed by 0-bits. The 1-bit is repeated every 72 samples, resulting in a single shaped pulse every 2 ms. The oscilloscope is triggered on the sync signal and set for 0.2 µs/div. The operator then sends commands to the DSK to alter the number of samples of delay between the transmitted and received signals. The sync signal, a short pulse, is output during the sample the DSK believes to be the center of the received bit. Thus the operator simply adjusts the delay value, which causes the

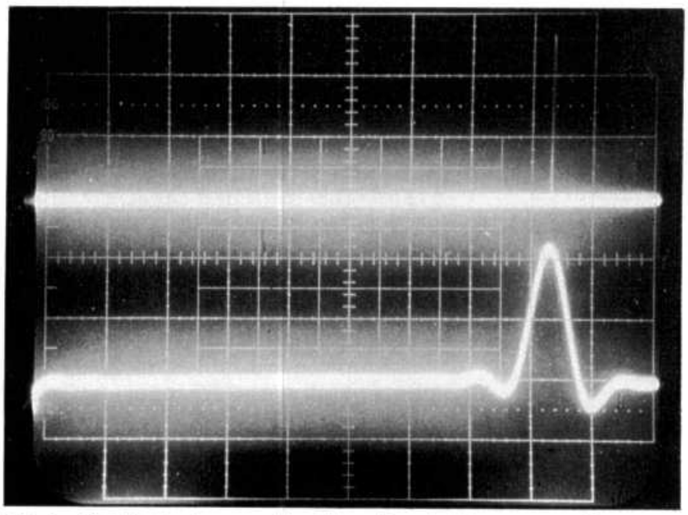

Fig 4—The first-phase calibration signal. When properly calibrated, the calibration signal (lower trace) is aligned with the sync pulse (upper trace) as shown. The oscilloscope is set for 0.2 µs/div. The sync pulse is very narrow and hard to see in this photograph but shows up well on the oscilloscope screen.

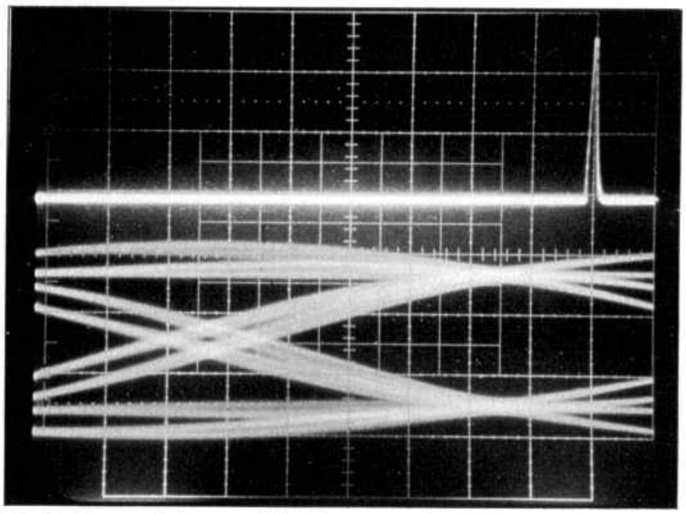

Fig 5—Second-phase calibration uses the BER test signal and sync pulse to produce an eye pattern. The oscilloscope is set for 10 µs/div. The center of the eye is adjusted to lead the sync pulse by 14 µs as shown.

received signal trace on the oscilloscope to move relative to the sync pulse. When the sync pulse is aligned with the shaped pulse of the received signal (Fig 4), the DSK is at the proper sample-delay value.

To achieve final calibration, the DSK clock phases must be adjusted to take into account the part of the system delay that is less than one sample period long. This is done by commanding the DSK to output its test signal and switching the oscilloscope to 10 µs/div. Now the oscilloscope displays a sync pulse at the right side of the screen, along with the *eye pattern* of the received data (Fig 5). The proper sampling point of the bits is the point where the eye is most "open." However, there is a 14-µs delay in the DSK system between the actual sampling point and the sync pulse. Thus, the operator commands the DSK to step its clock phase until the center of the eye leads the sync pulse by 14 µs. This is not a hugely critical setting—a few-microsecond error isn't normally detectable in the measured BER. The delay does have to be in the ballpark, however.

There is one more detail to consider during calibration. Depending on the system being tested, the received signal may be inverted from the transmitted signal; the positive-going pulses we sent may now be negative-going. If this is the case, the DSK will count all the correctly received bits as bad and all the bad bits as correct. So, the DSK supports a user command to invert the sense of the received data. The polarity of the received signal is most easily seen during the first calibration phase (Fig 4), and if the pulse is seen to be inverted then, the DSK's "invert" command should be issued. That will cause no difference in the displayed signal, but the DSK will know "which way is up."

DSP Program Operation

The DSP program used to perform BER measurements is called DBERT. The object file, DBERT.DSK, is downloaded into the DSK from the host computer. Once DBERT is running, it communicates with the host computer via the DSK's serial port. The serial I/O communication mechanism was described in a previous article.[2] When serial I/O is occurring, the DSP interrupts must be disabled. This keeps the DSP from executing its signal-processing operations during serial I/O. For that reason, DSK operation is controlled by the host computer using a command-response sequence: The host sends a command to the DSK, the DSK executes that command—including any needed signal processing—and reports completion of the command back to the host, if needed. Each command to the DSK from the host is a single ASCII character. Some commands result in the DSK needing to send data back to the host. In that case, once the command is completed by the DSK, it sends the data back to the host via the serial interface. Table 1 lists the commands supported by the DBERT program.

Because the DSK has to stop its signal I/O while communicating with the host, there is a potential problem in taking a measurement. When the DSK begins generating the test signal, it is possible that the system being tested will exhibit a response to the start-up transient from the DSK that invalidates the result. So, the BER test signal is started and the DSK waits 20,000 samples (about a half-second) before starting to sample the received signal.

We wanted to be able to test at consistent signal-to-noise ratios in order to establish reference levels for comparing different radios to one another. Since each unit will exhibit a unique sensitivity, we needed some way of adjusting the input power level to get a fixed output signal-to-noise ratio. The solution was to include a SINAD measurement function in the DBERT program. When the DSK receives the SINAD command from the host, it generates a 1-kHz sine wave. About a half-second after it begins generating the sine wave, the SINAD measurement software begins sampling the input signal. It then takes 8192 samples for measurement. Each measured sample is squared and added to a running sum (the *signal-plus-noise* value). The samples are also run through a narrow 1-kHz IIR notch filter that removes the 1-kHz test signal, leaving only the noise. The output samples from this filter are also squared and added to a (separate) running sum (the *noise* value). After 8192 samples have been processed, the two 32-bit sum values are returned to the host computer. The host can then calculate the SINAD by expressing the ratio of the signal-plus-noise value to the noise value in dB. A more detailed description of this technique was published in an earlier *QEX* article.[3]

The analog I/O of the DSK is performed by a TLC32040 integrated analog subsystem. This chip includes a 14-bit D/A, 14-bit A/D, sample-clock generator and input and output programmable switched-capacitor filters (SCF). The TLC32040 is driven by a 10-MHz clock produced by the processor chip. The frequency of this clock, in combination with the programmable dividers in the analog chip, determines the available sampling rates. The design of the BER test software calls for a 38,400 sample-per-second (sps) rate. Unfortunately, this exact rate isn't possible with the 10-MHz clock. The nearest available rate is approximately 38,461.5 sps. This translates to a 0.16% error in the speed of the test signals, which is negligible in the context of BER measurements. However, this error is suf-

Table 1—DBERT Commands

Command	*Return value*	*Description*
I	None	Generates test BER signal
C	None	Generates calibration signal
4	Error count (2 words)	Performs 10,000-bit BER test
5	Error count (2 words)	Performs 100,000-bit BER test
+	None	Increment sample delay
-	None	Decrement sample delay
A	None	Advance clock phase
0	None	Normal data polarity
1	None	Inverted data polarity
N	None	Generate 1-kHz sine wave
Q	None	Quiet (DSK output = 0 V)
S	SINAD value (4 words)	Take SINAD measurement
V	Input voltage (1 word)	Report input voltage value
T	None	Generate test signal (4800-Hz sine wave)

ficient to make the test signal unreadable by a G3RUH modem since the clock-recovery loop in that design has a very narrow lock range. I discovered this early on in the development of this system. To check that the problem was in fact the speed difference and not some problem with the signal I was generating, I temporarily removed the 40-MHz master oscillator on the DSK board—from which the 10-MHz clock is derived—and connected a signal generator to the clock input through a Schmitt trigger inverter. By setting the signal generator to generate exactly the clock frequency needed to get a 9600-baud signal, I found that the G3RUH modem was quite happy to consider my BER test signal a proper one.

Another problem with the TLC32040 is that the input SCF is a band-pass filter that normally cuts off at about 300 Hz. While the filter cutoff frequency is programmable, it can't be set anywhere near the very low frequency needed for this application. So, the DBERT program configures the TLC32040 to operate without its input filter. This requires that an external antialiasing filter be added. As shown in Fig 2, and described in more detail later, an SCF that cuts off at 10 kHz was added to the BER test box to fill this need.

The final characteristic of the TLC32040 to note is that it includes no internal sin*x*/*x* correction—not surprising in a chip with a programmable sample rate. Fortunately, with a sampling rate of 38400 Hz and signals of only up to 7200 Hz, the sin*x*/*x* roll-off at the upper end of the signal spectrum is only about ½ dB. Still, this seems worth correcting. The TLC32040 data sheet describes a first-order IIR filter that can be used to perform this correction. The *Mathcad* worksheet of Fig 6 shows the calculation of the coefficients of this sin*x*/*x* correction filter, which is implemented in the DBERT program. Fig 6 also shows the predicted output response both before and after the correction, as well as the estimated group delay of the correction filter.

As noted, the calibration procedure requires a sync pulse. The DSK has no uncommitted output signal lines usable for outputting a pulse, so DBERT outputs the sync pulse on the serial data output line. Since the sync pulse is less than a microsecond long, this won't usually bother the serial I/O chip of the host computer. (We did find one computer that was occasionally confused by the presence of the sync pulse.) The RS-232 signal is available on one of the DSK's expansion connectors. A 10-kΩ resistor connected to this point brings the sync signal out to the front panel of the BER test box. The presence of the resistor protects the RS-232 line from accidental shorting or application of another signal.

Host Application Software

We used two different programs. One, which we won't cover in detail here, manages the Lab's computer-controlled signal generator for

$f_s := 38400$ Sampling frequency $\quad f := 4800$ Upper frequency of passband

$f_n := \frac{f}{f_s} \quad f_n = 0.125$ Normalized upper frequency

$A := \left(\frac{\pi \cdot f_n}{\sin(\pi \cdot f_n)}\right)^2 \quad A = 1.0530293$ Amplitude correction at f_n

$f_L := \frac{1}{f_s} \quad f_L = 2.6041667 \cdot 10^{-5}$ Normalized lower passband frequency

$A_L := \left(\frac{\pi \cdot f_L}{\sin(\pi \cdot f_L)}\right)^2 \quad A_L = 1$ Amplitude correction at f_L

Compute needed first-order IIR coefficients

$p_1 := 1 \quad p_2 := 2$

Given

$$A \cdot \left(1 - 2 \cdot p_1 \cdot \cos(2 \cdot \pi \cdot f_n) + p_1^2\right) - p_2^2 \cdot (1 - p_1)^2 = 0$$

$$A_L \cdot \left(1 - 2 \cdot p_1 \cdot \cos(2 \cdot \pi \cdot f_L) + p_1^2\right) - p_2^2 \cdot (1 - p_1)^2 = 0$$

$$\begin{pmatrix} v_1 \\ v_2 \end{pmatrix} := \mathrm{Find}(p_1, p_2)$$

$v_1 = 0.1049616 \quad v_2 = 1$

Resulting first-order IIR filter: $y[n]=v_2(1-v_1)x[n]+v_1y[n-1]$

Computation of Corrected System Response

$$S(f) := \frac{\sin\left(\pi \cdot \frac{f}{f_s}\right)}{\pi \cdot \frac{f}{f_s}} \qquad M(f) := \frac{v_2 \cdot (1 - v_1) \cdot \exp\left(j \cdot 2 \cdot \pi \cdot \frac{f}{f_s}\right)}{\exp\left(j \cdot 2 \cdot \pi \cdot \frac{f}{f_s}\right) - v_1}$$

$P(f) := \arg(M(f))$

$f_x := 1, 70 .. 7000 \qquad \omega_x := 2 \cdot \pi, 70 \cdot 2 \cdot \pi .. 7000 \cdot 2 \cdot \pi$

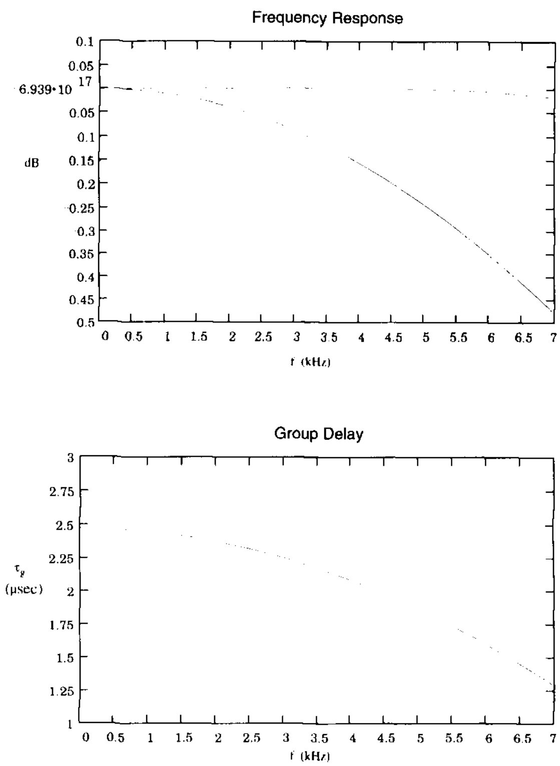

Fig 6—Correction of sin*x*/*x* roll-off is performed with a first-order IIR filter having the coefficients calculated by this *Mathcad* worksheet.

stepped BER measurements at various signal levels and frequencies. The other program, BERT.EXE, is a C program that communicates with the DSK under operator control. Communication with the DSK is normally performed at 19,200 baud, although slower speeds can be used. To ensure that no serial overruns occur, BERT uses interrupt-driven serial I/O.

The BERT program is quite straightforward. It accepts keyboard commands from the operator and sends them to the DSK. The command set is the same as that of DBERT—BERT just passes these commands through to the DSK—with a couple of additions. Also, BERT "knows" about those DSK commands that generate a response from DBERT. When such a command is given, BERT waits for the response from the DSK, then converts the incoming serial bytes to binary values. In the case of BER test values (commands *4* and *5*), it prints out the reported number of errors and the BER, calculating the latter based on the number of bits the DSK was commanded to use in its test. For the SINAD command (*S*), BERT computes and prints the SINAD and the distortion percentage using the values returned by DBERT.

The DBERT program can perform BER tests using 10,000 samples or 100,000 samples. The BERT program also provides a 1-million sample BER test (the *6* command), which it performs by commanding the DSK to perform a 100,000-sample BER test 10 times. BERT sums the values from each of these tests to get the final result. As each BER test result is returned from the DSK, BERT prints the running total of samples, errors and BER. The *L* command performs the same function, except that it stops if 100 or more total errors have been reported.

If the operator selects the calibrate (*C*), idle (*I*), sine-wave (*N*) or quiet (*Q*) commands, BERT remembers the selected command. Whenever a BER or SINAD test command is performed, BERT waits for that command to complete, then sends the appropriate command to place DBERT in the most recently selected mode from among those listed.

BER Test Box Hardware

The BER test box contains several op-amp amplifiers used to keep the input signals within the range of the TLC32040 analog input. The box also contains a mixer and a demodulator, shown in Fig 2, designed by ARRL Lab Engineer Zack Lau, KH6CP. To test transmitters, the transmitter output is attenuated with a high-power attenuator down to a level that the SBL-1 mixer, U3, can handle. The LO input of the SBL-1 is driven by a +7-dBm signal from a signal generator set to a frequency 373-kHz below or above the transmitter frequency. The output from the SBL-1 passes through a low-pass filter that removes the sum frequency, leaving only the 373-kHz difference frequency. This signal is applied to an NE604 FM IF chip that contains a limiter, IF amplifier and quadrature FM demodulator. The frequency at which the demodulator operates is set by L1 and its associated silver-mica capacitor. When Zack built this circuit, the components he used just happened to fall at 373 kHz. If you reproduce the circuit, it's likely that your copy will work at a slightly different frequency. This shouldn't present a problem; the exact operating frequency isn't critical.

Since the NE604 operates from a single 5-V supply, its output is a positive voltage. This signal is fed into U4A, which amplifies the signal and also removes the positive offset, so that the result is zero volts when the input signal is at 373 kHz. U4B amplifies this demodulated signal or an external input signal (usually the output of a receiver being tested) with adjustable gain. The signal is finally filtered in an MF4 4th-order Butterworth low-pass SCF, U6, that acts as the antialiasing filter for the DSP input. The cut-off frequency of U6 is determined by its input clock, with the clock being 50 times the cutoff frequency. In our test set, this clock is supplied by an external function generator, but it could as easily be provided by a crystal oscillator and divider chain.

Interpreting BER Measurements

Bit errors are (or should be) due mainly to corruption of the signal by noise. Thus, they should be random. That being the case, if you make the same measurement several times, you are likely to get different results each time. But the more bits you send through the system, the more the effect of noise is averaged and the more consistent the measurements will be. That raises the question: How many bits do you need to use to get a valid result? The answer to that question depends on what you mean by "a valid result." The more bits you use, the closer your measurement will be to the "true" BER you would get if you sent an *infinite* number of bits through the system. Since sending an infinite number of bits through the system is a little, well, impractical, we need to come up with some guidelines for selecting a finite number of bits to use.

Unfortunately, in order to do that we have to make some assumptions about the character of the noise in the system. Fortunately, the assumptions we make hold up pretty well for real systems. (There's nothing new about this; we make assumptions about the character of system noise all the time. For example, when we relate noise to system bandwidth we often assume that the noise is uniformly distributed across the spectrum of interest.)

What we find is that with a given number of bits in the sample set, and a given number of errors within those bits, we can establish a *confidence interval*. The confidence interval tells us how likely it is that our measurement is within some specified factor of the "true" BER. For example, we might find that our measurement gives us an 80% confidence that the value is within a factor of 3 of the true BER. The end result is that we can get as good a measurement as we want if we are willing to wait for enough bits to go through the system. Of course, at a low BER we don't get many errors, so we need to send a *lot* of bits!

What's interesting about the confidence interval is that it depends on the number of errors detected. Suppose you made two BER measurements. If for the second measurement you double the number of bits sent and get double the number of errors, you end up with the same BER but a higher confidence. On the other hand, if you double the number of bits but measure the same number of errors (you're measuring at a lower noise level, for instance), you get a lower BER but the same confidence interval. What that means is that all we need to do is to ensure that we have at least the number of errors needed to establish the desired confidence interval.

There are two useful sets of numbers we've used here in the ARRL Lab for our BER testing. If you measure 10 bit errors, you are 95% sure that you are within a factor of about 2 of the true BER. And if you get 100 bit errors, you are 99% sure that you are within a factor of about 1.3 of the true BER.[4] If you look at a curve of BER versus signal-to-noise ratio, you'll find that a factor-of-2 difference in BER occurs with a fraction of a dB change in signal-to-noise ratio. That suggests that a measurement that results in 10 bit errors is a pretty good one, and a measurement that results in 100 bit errors is a *very* good measurement. That's why the *L* command exists in the BERT program. It pops 100,000 bits at a time through the system, stopping when 100 or more errors have been reported—because continuing to measure more bit errors is a waste of time—or when 1 million bits have been sent. Using a million bits means that a BER of 1×10^{-4} (100 bit errors) or worse can be measured with great accuracy, and a BER of 1×10^{-5} (10 bit errors) can be measured with decent accuracy. Of course, if you have time on your hands you can measure a BER of 1×10^{-6} by sending 10 million bits through the system. (That takes over 17 minutes at 9600 baud!)

Conclusion

The system described here has been used to measure a number of 9600-baud radios. Some of the test results will be presented in an upcoming *QST* article, and future *QST* reviews of 9600-baud radios will include measurements made using this system. The system has proven to be effective and easy to use. I should add that we spot-checked the results obtained with this system by measuring BER using a G3RUH modem. It gave BER results that were consistently slightly better because its input filter cuts off at a lower frequency than the SCF in the BER test box, improving the signal-to-noise ratio.

The software for this system, including the source code, is available for downloading from the ARRL BBS (203-666-0578) and via the Internet using anonymous FTP from ftp.cs.buffalo.edu. The file name is QEXBERT.ZIP.

Notes

[1]Couch, L. W., *Digital and Analog Communication Systems* (New York: Macmillan, 1993), p 179.

[2]Bloom, J., KE3Z, "Measuring System Response with DSP," *QEX*, February 1995, pp 11-23.

[3]Bloom, J., KE3Z, "Measuring SINAD Using DSP", *QEX*, June 1993, pp 9-13.

[4]Jeruchim, M. C., Balaban, P. and Shanmugan, K. S., *Simulation of Communication Systems* (New York: Plenum Press, 1992), pp 492-501.

Upcoming Technical Conferences

40th Annaul West Coast VHF/UHF Conference

May 5-7, 1995, Sheraton Cerritos Hotel, Town Center, 12725 Center Court Drive, Cerritos, California.

For more information please call 714-990-9203 or fax 714-990-1340.

1995 ARRL Digital Communications Conference

September 8-10, 1995, La Quinta Conference Center, Arlington, Texas—just minutes from Dallas/Fort Worth Airport. Co-hosted by Tucson Amateur Packet Radio (TAPR) and the Texas Packet Radio Society.

More information will be released soon, or contact the TAPR office at 8987-309 E. Tanque Verde Road #337, Tucson, AZ 85749-9399, tel: 817-383-0000; fax: 817 566-2544; Internet: tapr@tapr.org

Call for papers: Deadline for receipt of camera-ready papers is **July 21, 1995**. Contact Maty Weinberg at ARRL HQ (tel: 203-666-1541; fax: 203-665-7531; Internet: lweinberg@arrl.org) for infomation on submitting papers.

Microwave Update 95

October 26-28, La Quinta Inn, Arlington, Texas.

For more information contact: Al Ward, WB5LUA, 2306 Forest Grove Estates Road, Allen, TX 75002 or Kent Britain, WA5VJB, 1626 Vineyard, Grand Prairie, TX 75052-1405.

RF

By Zack Lau, KH6CP/1

Calculating the Power Limit of Circuits with Toroids

A notable black hole in RF design is the calculation of how much power toroidal inductors can handle. The reason is pretty obvious—just look at books like Grover's *Inductance Calculations* to see how difficult it is to solve the "easy" cases, without the complications of real RF circuits such as skin and proximity effects.[1] On the other hand, even a rough approximation is better than nothing, especially for those without practical experience on which to base a guess, uh, estimate.

The approach is as follows. First, measure the Q of each inductor at the operating frequency. Next, using the measured Q values, analyze the circuit and calculate the current through each inductor as a function of the input power. (Computer modeling is useful, but not essential. Matrix algebra will handle the most commonly used networks.) This will let you calculate the power lost by the inductor. Finally, relate the power loss to a surface temperature rise. That's what we want to know: how much power makes the inductors too hot?

[1]Notes appear on page 25.

225 Main Street
Newington, CT 06111
email: zlau@arrl.org

Actually, you can get acceptable results by guessing the Q. If you think the Q will be low, guess 100. If you think it will be high, guess 300. This works well for the type-2 and type-6 iron-powder materials used at HF. (If you are thinking about using type-1 material at 160 meters, don't—use type-2 material instead. Apparently, the core loss of type-1 material offsets the decrease in copper loss, so the only advantage is the fewer turns required.) Another source of Q values is the charts in the Amidon booklet, *Iron-Powder and Ferrite Coil Forms*.[2] Of course, the preferred method is to measure the Q at the frequency of operation. The charts show that the Q will be optimum at a particular frequency and degrade as you move away. A set of equations for calculating this would make an excellent *QEX* article by someone who wants a challenge!

If you are fortunate enough to have a Q meter, you can just set the frequency and make the measurement. But you can also measure Q with simple equipment. Just measure the bandwidth and insertion loss of a filter and use this to calculate the Q of the components involved. If you want simplicity, you can use very light coupling so that the measured Q approaches the inductor Q. You can ignore the loss of the capacitors to make the math easier, although this isn't necessary if you are using a computer modeling program such as *ARRL Radio Designer* (*ARD*). In any case, ignoring the capacitor loss will add a safety factor by making the Q of the inductor appear slightly worse than it actually is.

Finally, for those of you who need some information right now, you might use the measurements I've listed in Table 1. I took this data over a number of years using a Hewlett-Packard 4342A Q meter. Unlike the equipment we use here in the ARRL Lab for product-review testing, the Q meter isn't calibrated on a regular basis. Still, the numbers should be reasonably useful.

If you wonder about the particular coil selection of Table 1, keep in mind that the goal was usually to quickly optimize Q given some constraints—it is hardly the measurement of random coils. Hopefully, more people will be willing to share their measured data with the amateur community to improve the quality of homebrew designs.

Example 1

The circuit in Fig 1 is a 3-element π network that transforms 50 Ω to 84.5 Ω at 14.1 MHz. My simplified analysis of the network by hand indicates that I_L is $V_1/42.8\ \Omega$. With a simple ladder or π network, the math is straightforward—it isn't necessary to resort to matrix algebra to get the loop currents. If you have a computer program such as *ARD*, you can model the inductor as an ideal inductor in series with a resistor. The power lost across the resistor is the power loss. It can be surprisingly high if you have a lot of circulating current. Keep in mind that *ARD* applies the voltage though the source resistance. Thus, if you set the source to 1 V (RMS), you are applying 5 mW to a matched circuit, not the 20 mW to the 50-Ω circuit one might expect.

Calculating the resistive loss in the circuit of Fig 1 gives:

$$R_S = 2\pi f L_1 / Q$$
$$= 62.9\,\Omega / 236$$
$$= 0.266\,\Omega$$

The power lost in this resistive component is:

$$P_{loss} = R_S I_L^{\,2}$$
$$= 0.266\,\Omega(V_1 / 42.8\,\Omega)^2$$

How much does the toroid heat up?

According to the Micrometals catalog, the temperature rise of a toroidal inductor is:

$$\Delta T = \left[\frac{\text{power loss (mW)}}{\text{surface area (cm}^2)}\right]^{0.833}$$

where ΔT is in °C.[3] Since it takes 2 hours for the core to stabilize at this temperature, this is quite conservative for most amateur applications. Normal amateur duty cycles will allow you to double or triple the allowable power loss.

The surface area is easily found in the reference data: the surface area of a T-50 core is 6.86 cm^2. If a 25 °C temperature rise is acceptable:

$$P_{loss} = (\text{surface area})(\Delta T)^{1.2}$$
$$= 6.86(25)^{1.2}$$
$$= 326\,\text{mW}$$

Thus, we now have a loss value from which calculate the allowable power input:

$$0.266\,\Omega(V_1 / 42.8\,\Omega)^2 = 326\,\text{mW}$$
$$V_1 / 42.8 = \sqrt{0.326 / 0.266}$$
$$V_1 = 47.4\,\text{V}$$

By comparison, *ARD* reports 0.00307 V across the inductor resistor when 0.496 V is across C1. Thus, P_{in} is 45.3 W according to the computer model. I think this is reasonably close.

Example 2

A tuned two-pole band-pass filter is usually designed for a narrow bandwidth. As a result, it isn't unusual to have a loss of 2 dB, or 37%. If the capacitor losses aren't a factor, 18.5% of the power is lost in each inductor. Thus, this circuit will only handle 1.8 W, using the same 25 °C temperature-rise criterion. Note that instead of going through all the work of calculating the actual current in the inductor, we have instead used the loss of the circuit. This is often easier to measure and calculate.

It can be argued that this isn't exactly correct—that for high-loss filters the loss in each inductor will be slightly different. Perhaps. But I'll point out that trying to get precision results is quite apt to result in answers that are entirely wrong because of mistakes made in the overly complicated analysis. For most of us, rough numbers that are easily calculated make more sense. After all, in real life each component will be slightly different.

How reasonable is the 25 °C temperature rise criterion? On a warm summer day, you might end up with a temperature of 55 °C, which is pretty warm to the touch. (Of course, smart RF experimenters know better than to touch circuits with lots of RF applied—RF burns do hurt!)

Another consideration is temperature stability. Type-6 iron-powder is one of the better materials, with a temperature coefficient of 35 ppm/°C. Thus, the inductance will only change by 880 ppm, or 0.088%. On the other hand, suppose your inductors were made out of type-67 ferrite, with a temperature coefficient of 0.13%/°C. A 25 °C rise would result in a variation of 3.2%, which can be quite noticeable if there is a large impedance transformation or if the circuit bandwidth is narrow. Also, magnetic materials have a Curie temperature at which they cease to be ferromagnetic. This is as low as 130 °C for type-43 ferrite material and as high as 500 °C for type-67 material. Micrometals, a company that makes iron-powder toroids, recommends that the toroids only be used between –55° and 125 °C, as "continued operation above 125 °C will generally result in a permanent decrease in both inductance and Q."[3]

Finally, you might wonder why I didn't mention any flux-density calculations. Since flux density is inversely proportional to frequency, saturating an inductor at 10 MHz is 1000 times as difficult as it is at 10 kHz. Thus, while it is a concern when designing switching power supplies, it is rarely a problem at RF.

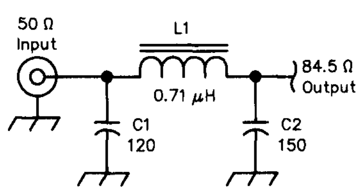

Fig 1—Schematic diagram of a 50 to 84.5-Ω π network at 14.1 MHz. L1—12 turns #22 enameled wire on a T-50-6 iron-powder toroid core. (0.71 µH, Q=236 at 14.1 MHz.)

An Inexpensive Dish Source

You can buy RCA DSS 18-inch dish parts from MCM Electronics, 650 Congress Park Drive, Centerville, OH 45459, tel: 1-800-543-4330, fax: 1-513-434-6959. (See p 209 of MCM's Catalog 34.) These 18-inch offset-feed dishes are inexpensive—one version of the steel reflecting surface is only $13.15, while an apparently reinforced version goes for $22. The mounting bracket is another $14.85. These are new replacement parts, so getting large quantities for club projects shouldn't be a problem. The offset-feed requirement complicates feed positioning slightly, as there are two positioning variables to deal with instead of one. But once someone comes up with a duplicable feed design, these dishes promise to be a low-cost route onto the microwave bands.

Notes

[1]Grover, F. W., *Inductance Calculations*, Dover Publications, ISBN 0-87664-557-0.

[2]Amidon Associates, PO Box 956, Torrance, CA 90508. Tel: 310-763-5770; fax: 310-763-2250.

[3]*RF Applications, Micrometals Iron Powder Cores*, Catalog 3 Issue D. Micrometals, Inc, 1190 N. Hawk Circle, Anaheim, CA 92807. Tel: 1-800-356-5977.

Table 1—Measured Toroidal Inductor Q Values

In the following list, the Q of some coils was measured at several frequencies. These measurements are grouped together, with only one of the values showing a measured inductance. The tracking code allows me to go back and check my notebook—everyone has at least one notebook, right?

L (uH)	*Q, f (MHz), turns, wire gauge, core, tracking code*
0.0885	64.5, 25.2, 10t, #24, T-25-0, 3p2
0.0931	114, 25.2, 5t, #24, T-16-6, 3p3
0.0949	111, 25.2, 5t, #26, T-16-6, 3p2
0.0975	116, 25.2, 4t, #24, T-37-6, 1p108
0.104	95, 25.2, 6t, #24, T-30-12, 3p78
0.1079	73, 25.2, 12t, #24, T-25-0, 3p2
0.111	130, 25.2, 5t, #24, T-37-10, 1p129
0.124	134, 25.2, 4t, #24, T-50-6, 1p108
0.127	114, 25.2, 6t, #28, T-16-6, 3p2
0.129	140, 25.2, 5t, #24, T-37-6, 1p108
0.139	102, 25.2, 5t, #24, T-25-2, 1p136
0.140	90, 25.2, 7t, #26, T-20-2, 1p136
0.158	107, 25.2, 7t, #26, T-20-6, 3p79
0.158	126, 25.2, 6t, #24, T-37-10, 1p129
0.17	99.9, 25.2, 6t, #24, T-25-2, 1p136
0.173	95, 25.2, 7t, #26, T-20-2, 1p136
0.180	136, 25.2, 5t, #24, T-50-6, 1p108
0.215	125, 25.2, 8t, #26, T-20-6, 3p79
0.215	152, 25.2, 6t, #24, T-37-2, 2p62
0.219	154, 25.2, 8t, #26, T-30-10, 2p58
0.220	146, 25.2, 6t, #24, T-50-6, 1p108
0.221	143, 25.2, 8t, #24, T-25-6, 2p47
0.23	170, 25.2, 6t, #22, T-44-6, 3p61
0.234	124, 25.2, 8t, #24, T-37-10, 2p62
0.234	177, 25.2, 7t, #24, T-30-6, 1p149
0.247	139, 25.2, 8t, #24, T-37-19, 1p129
0.258	178, 25.2, 7t, #24, T-30-6, 2p62
0.269	167, 25.2, 8t, #24, T-37-6, 2p62
0.27	177, 25.2, 7t, #22, T-50-6, 3p69
0.275	143, 25.2, 9t, #24, T-25-6, 2p47
0.276	147, 25.2, 9t, #24, T-25-6, 2p51
0.285	104, 25.2, 10t, #26, T-20-2, 1p136
0.30	167, 25.2, 10t, #26, T-30-10, 2p58
0.303	164, 25.2, 9t, #24, T-37-6, 2p62
0.31	172, 25.2, 7t, #22, T-50-6, 3p68
0.325	170, 25.2, 8t, #24, T-30-6
0.332	105, 25.2, 11t, #26, T-20-2, 1p136
0.342	115, 25.2, 9t, #26, T-25-2
0.36	142, 25.2, 9t, #28, T-25-6
0.36	172, 25.2, 11t, #24, T-37-10, 1p129
0.362	106, 25.2, 9t, #26, T-25-2
0.362	122, 25.2, 9t+1/2, inch, lead, #26, T-25-2
0.37	183, 25.2, 8t, #22, T-50-6, 3p68
0.38	163, 25.2, 10t, #24, T-37-6, 2p62
0.40	169, 25.2, 9t, #26, T-30-6, 3p79
0.42	116, 25.2, 10t, #26, T-25-2
0.43	146, 25.2, 12t, #26, T-25-6, 2p39,
0.44	166, 25.2, 11t, #24, T-37-6, 2p62,
0.45	146, 25.2, 13t, #28, T-20-6, 1p150
0.47	172, 25.2, 9t, #20, T-44-6
0.47	189, 25.2, 9t, #20, T-44-6
0.489	186, 25.2, 10t, #24, T-30-6, 2p48
0.49	174, 25.2, 11t, #24, T-37-10, 1p129, close wound
0.49	146, 25.2, 12t, #26, T-25-6, 2p39
0.49	151, 25.2, 14t, #28, T-16-6

L (uH)	*Q, f (MHz), turns, wire gauge, core, tracking code*
0.495	223, 14.1, 10t, #22, T-50-6, 2p7
	223, 18.1
	216, 21.2
	200, 25.2
	182, 28.5
0.58	188, 25.2, 12t, #24, T-37-6, 3p70
0.59	209, 25.9, 11t, #20, T-50-6, 1p118
	188, 28.5
	270, 18.1
	256, 21.2
	235, 24.5
0.62	231, 25.2, 9t, #20, T-68-6, 1p118
	208, 28.5
0.63	183, 25.2, 12t, #24, T-30-6, 1p150
0.65	190, 25.2, 12t, #24, T-20-6, 1p150
0.66	180, 25.2, 12t, #26, T-30-6, 2p45
0.67	185, 25.2, 13t, #24, T-37-6, 3p70
0.67	192, 25.2, 14t, #22, T-37-6, 2p39
	237, 10.1
	246, 14.1
	242, 18.0
	232, 21.0
0.69	210, 25.2, 11t, #20, T-50-6, 50% coverage, 1p118
	189, 28.5, see 0.59
0.71	132, 25.2, 11t, #24, T-37-2
0.71	227, 10.1, 12t, #22, T-50-6, 2p7
	236, 14.1
	232, 18.1
	222, 21.1
	201, 24.9
	200, 25.2
	178, 28.5
0.72	183, 25.2, 15t, #22, T-37-6, 2p39
	182, 10.1
	188, 14.0
	188, 18.0
	186, 21.0
0.72	195, 25.2, 13t, #24, T-30-6, 1p150
0.73	179, 25.2, 13t, #24, T-30-6, 1p150
0.74	181, 25.2, 13t, #24, T-30-6, 1p150
	182, 10.1
	188, 14.0
	188, 18.0
	186, 21.0
	179, 24.5

L (uH)	Q, f (MHz), turns, wire gauge, core, tracking code
0.74	177, 25.2, 14t, #20, T-50-10, 1p118
	172, 28.5
0.75	195, 25.2, 13t, #24, T-30-6, 1p150
0.75	194, 25.2, 13t, #24, T-30-6
0.75	188, 25.2, 12t, #22, T-50-6
0.76	185, 25.2, 13t, #24, T-30-6
0.76	192, 25.2, 12t, #20, T-44-6
0.78	163, 25.2, 14t, #28, T-37-6, 1p149
0.79	147, 25.2, 18t, #30, T-20-6, 1p150
0.79	149, 25.2, 18t, #30, T-20-6, 1p150
0.79	122, 25.2, 12t, #24, T-37-2
0.79	194, 25.2, 12t, #22, T-50-6, 3p68
0.80	148, 25.2, 18t, #30, T-20-6, 1p150
0.80	113, 25.2, 13t, #24, T-37-2, 1p135
0.81	120, 7.9, 13t, #24, T-37-2, 1p135
0.82	148, 25.2, 18t, #30, T-20-6, 1p150
	220, 10.1
	234, 14.1
	228, 21.0
	212, 24.9
0.83	211, 25.2, 15t, #24, T-37-6, 1p131
	196, 28.0
0.83	188, 25.2, 14, t, #24, T-30-6, 1p150
0.853	166, 7.9, 11t, #22, T-50-2, 3p68
0.86	162, 7.9, 13t+lead, #24, T-37-2
0.878	243, 7.9, 13t, #20, T-50-6, 1p118
	255, 10.1
	260, 14.1
	237, 21.0
0.88	210, 25.9
	188, 28.5
	233, 7.1, 0.869, 286, 7.9
	294, 10.1
	286, 14.1
	266, 18.1
	246, 21.0
	218, 24.5
0.88	212, 25.2, 12t, #16, T-68-6, 1p118
	186, 28.5
0.91	166, 25.2, 15t, #28, T-37-6, 1p149
0.918	202, 7.9, 12t, #22, T-44-2, 3p89
0.93	130, 25.2, 13t, #24, T-37-2
0.93	191, 7.9, 12t, #22, T-50-2, 2p65
0.931	145, 7.9, 18t, #30, T-20-2, 2p4
	150, 10
	148, 14
	138, 18
	128, 21
0.932	232, 7.9, 14t, #22, T-50-6, 2p7
	240, 10.1

L (uH)	Q, f (MHz), turns, wire gauge, core, tracking code
	245, 14.1
	236, 18.1
	223, 21.2
	198, 24.9
	174, 28.5
	290, 10.1
	294, 14.1
	280, 18.1
	236, 24.5
0.94	232, 25.9, 12t, #20, T-68-6, 1p118
	206, 28.5
0.95,	172, 7.9, 14t, #24, T-37-2
0.965	183, 7.9, 12t, #22, T-44-2, 3p89
0.97	168, 7.9, 12t, #22, T-50-2, 3p68
0.98	166, 25.2, 16t, #28, T-37-6, 1p149
0.99	167, 7.9, 16t, #26, T-25-2, 2p4
	168, 10.1
	160, 14
	144, 18
	132, 21
1.03	214, 7.9, 17t, #24, T-37-6, 1p131
	228, 10.1
	241, 14.0
	232, 21.0
	214, 24.9
	197, 28.0
1.038	213, 7.9, 16t, #24, T-30-6, 1p149
1.05	169, 7.9, 17t, #26, T-30-2, 2p4
	173, 10
	168, 14
	167, 7.3
1.06	270, 7.9, 15t, #20, T-50-6, 2p12
	283, 10.1
	283, 14.2
	268, 18.1
	250, 21.0
1.065	173, 7.9, 13t, #22, T-50-2, 3p68
1.105	182, 7.9, 15t, #24, T-37-2
1.12	255, 7.9, 15t, #20, T-50-6, 1p118
	265, 10.1
	270, 14.1
	242, 21.1
	210, 24.5
	182, 28.5
1.13	180, 7.9, 15t, #24, T-37-2
1.165	238, 7.9, 16t, #22, T-50-6, 2p13
	249, 14.2
	237, 18.1
	224, 21

L (uH)	Q, f (MHz), turns, wire gauge, core, tracking code
	293, 7.0
	300, 10.1
	285, 14.1
	255, 18.1
	228, 21.2
1.2	194, 25.2, 14t, #20, T-68-7, 1p118
	167, 28.5
1.22	215, 7.9, 19t, #24, T-37-6
	157, 28.0
1.22	225, 7.9, 19t, #24, T-37-6, 2p12
	190, 24.9
	170, 28.0
1.22	215, 7.9, 14t, #22, T-50-2, 2p65
1.23	215, 7.9, 19t, #24, T-37-6, 2p12
	187, 24.9
	168, 28.0
1.23	188, 7.9, 16t, #24, T-37-2
	226, 7.1
1.23	233, 7.9, 16t, #22, T-50-6, 2p12
	241, 10.1
	240, 14.2
	226, 18.1
1.255	238, 7.9, 16t, #22, T-50-6, 2p7
	231, 7.1
	247, 10.1
	248, 14.2
	234, 18.1
	217, 21.2
	191, 24.9
	215, 7.1
1.26	224, 7.9, 19t, #24, T-37-6, 1p131
	237, 10.1
	248, 14.0
	215, 24.9
	196, 28.0
1.28	176, 7.9, 16t, #24, T-37-2, evenly spaced
1.28	241, 7.1, 16t, #22, T-50-6, 2p11
	247, 7.9
	256, 10.1
	255, 14.2
	242, 18.1
	225, 21.2
1.3	260, 14, 17t, #22, T-50-6, 2p12
1.32	250, 14, 17t, #22, T-50-6, 2p12
1.33	237, 7.1, 16t, #22, T-44-6, 2p7
	243, 7.9
	248, 10.1
	241, 14.1

L (uH)	Q, f (MHz), turns, wire gauge, core, tracking code
	222, 18.1
	202, 21.2
	322, 7.1
1.34	332, 7.9, 15t, #20, T-68-6, 1p118
	342, 10.1
	335, 14.1
	309, 18
	280, 21.2
1.36	177, 7.9, 17t, #24, T-37-2
1.36	282, 14, 15t, #22, T-68-6, 3p99
	278, 7.9
1.39	218, 7.9, 15t, #22, T-44-2, 3p89
1.39	185, 7.9, 15t, #22, T-44-2, 2p65
1.4	253, 7.9, 17t, #22, T-50-6
1.43	246, 7.1, 17t, #22, T-50-6, 2p11
	252, 7.9
	259, 10.1
	256, 14.2
	230, 18.1
	222, 21.2
1.43	225, 7.9, 15t, #22, T-50-2, 2p65
1.44	182, 7.9, 17t, #26, T-30-2
1.44	192, 7.9, 17t, #24, T-37-2
1.44	225, 7.9, 21t, #24, T-37-6, 2p12
	183, 24.9
	164, 28.0
1.45	228, 7.9, 21t, #24, T-37-6
	238, 10.1
	238, 14.2
	226, 18.1
	209, 21.2
	184, 24.9
	163, 28.0
1.57	180, 7.9, 19t, #22, T-50-2, 1p102
	168, 10.1
	144, 14.0
1.58	190, 7.9, 18t, #24, T-37-2
	230, 7
1.67	237, 7.9, 22t, #24, T-37-7, 1p101
	248, 10
	237, 14
	213, 18
1.69	240, 7.9, 18t, #20, T-50-2
1.75	217, 25.9, 21t, #26, T-30-6, 2p53
1.78	181, 7.9, 20t, #, 24, T-37-2,
1.79	170, 7.9, 19t, #24, T-44-2

L (uH)	Q, f (MHz), turns, wire gauge, core, tracking code
1.8	231, 7.9, 17t, #22, T-50-2, 2p65
	335, 7.1
1.82	342, 7.9, 18t, #20, T-68-6, 1p117
	348, 10.1
	330, 14.1
	260, 21.2
1.86	167, 7.9, 22t, #30, T-25-2, 2p4
	164, 7.1
	168, 10.1
	162, 14.0
	147, 18.0
	134, 21.0
2.0	172, 7.9, 23t, #30, T-25-2, 2p4
	168, 7.1
	172, 10.1
	163, 14.0
	147, 18.0
	134, 21.0
	335, 7.1
2.04	335, 7.9, 19t, #18, T-68-7, 1p129
	325, 10.1
	278, 14.2
	236, 18.1
2.1	225, 7.9, 19t, #24, T-44-2
2.12	286, 7.9, 12t, #18, T-130-2
2.15	280, 7.9, 13t, #18, T-130-2
	229, 7.0
2.2	227, 7.9, 19t, #22, T-50-2, 1p127
	219, 10.1
2.25	231, 7.9, 19t, #22, T-50-2, 2p65
2.34	287, 7.9, 13t, #18, T-130-2
2.4	220, 7.9, 25t, #28, T-30-6, T-30-6, 1p149
2.44	168, 7.9, 22t+1", #28, T-30-2, 3p81
2.44	223, 7.9, 20t, #24, T-44-2
	268, 7.1
2.47	271, 7.9, 24t, #22, T-50-6, 2p12
	269, 10.1
2.52	262, 7.1, 24t, #22, T-50-6, 2p11
	263, 7.9
	260, 10.1
	233, 14.2
2.62	227, 7.9, 21t, #24, T-44-2
2.63	168, 7.9, 23t, #28, T-30-2, 3p81
2.63	191, 7.9, 22t, #22, T-50-2, 2p66
	330, 5.0
	335, 5.0
	345, 7.0
2.7	343, 7.9, 11t, #20, bifilar, T-68-6, 1p79

L (uH)	Q, f (MHz), turns, wire gauge, core, tracking code
	332, 10
	330, 10.5
	275, 14
	221, 18
2.72	222, 7.9, 30t, #26, T-37-6, 2p54
2.82	172, 7.9, 24t, #28, T-30-2, 3p81
2.82	212, 7.9, 25t, #26, T-37-2, 3p55
	281, 7.1
2.85	282, 7.9, 26t, #22, T-50-6
	282, 10.1
	268, 7.1
2.86	267, 7.9, 26t, #22, T-50-6, 2p13
	257, 10.1
2.9	272, 7.1, 26t, #22, T-50-6, 2p11
	273, 7.9
	267, 10.2
	233, 14.2
2.91	225, 7.9, 23t, #22, T-50-2, 1p127
3.0	232, 7.9, 26t, #22, T-50-2, 1p127
3.07	239, 7.9, 24t, #22, T-50-2, 2p65
3.08	222, 7.9, 24t, #22, T-50-2, 2p65
3.1	228, 7.1, 24t, #22, T-50-2, 2p11
	224, 7.9
	209, 10.1
	175, 14.2
3.13	195, 7.9, 26t, #26, T-37-2
	247, 7.1
3.19	242, 7.9, 24t, #22, T-50-2, 1p127
	225, 10.0
	300, 7
3.25	300, 7.9, 26t, #20, T-80-6, 1p78, see 3.4, bifilar
	290, 10
	290, 10.5
	260, 14
3.27	192, 7.9, 28t, #26, T-37-2, 1p136
	239, 7
3.29	254, 7.9, 31t, #26, T-37-7, 1p101
	248, 10
	237, 14
	213, 18
3.35	202, 7.9, 27t, #26, T-37-2
3.36	182, 7.9, 28t, #26, T-37-2, 1p136
	291, 5.0
	299, 5.2
	309, 5.4
	315, 6
	320, 7

L (uH)	Q, f (MHz), turns, wire gauge, core, tracking code
3.4	320, 7.9, 13t, bifilar, #20, T-80-6, 1p78
	310, 10
	309, 10.5
	280, 13
	265, 14
3.5	233, 4.0, 25t, #22, T-50-2, 2p11
	231, 7.1
	226, 7.9
	209, 10.1
	172, 14.2
3.6	183, 7.9, 28t, #28, T-30-2
3.6	204, 7.9, 26t, #24, T-44-2, 2p47
3.7	210, 7.9, 26t, #24, T-44-2, 2p47
3.75	210, 7.9, 26t, #25, T-44-2, 3p2
3.9	202, 7.9, 26t, #24, T-44-2
4.2	216, 7.9, 27t, #24, T-44-2
4.2	204, 7.9, 27t, #24, T-44-2
5.2	263, 7.9, 19t, #18, T-225-2
5.4	350, 7.9, 26t, #18, T-94-6, 2p2
5.4	273, 7.9, 19t, #18, T-225-2
5.5	195, 7.9, 34t, #30, T-30-2
	335, 5
5.6	330, 7.9, 33t, #22, T-68-6, 1p98
5.8	271, 7.9, 20t, #18, T-225-2
5.81	197, 7.9, 35t, #30, T-30-2
5.9	224, 7.9, 35t, #24, T-50-2, 2p38, see 6.7 & 6.4
	232, 3.5
	243, 3.6
	244, 3.8
	245, 4.0
	183, 10.0
	183, 14.1
	184, 18.0
	182, 21.0
6.0	176, 25.9, 12t, #20, T-50-10, 1p118
	171, 28.5
6.1	217, 7.9, 34t, #24, T-50-2, 2p13,
	236, 3.5
	237, 3.6
	238, 4.0
6.25	212, 7.9, 34t, #24, T-50-2, 2p13,
6.3	213, 7.9, 34t, #24, T-50-2, 3p9
	152, 12.4

L (uH)	Q, f (MHz), turns, wire gauge, core, tracking code
6.4	206, 7.9, 35t, #24, T-50-2, 2p38, see 5.9 & 6.7
	461, 3.4
	462, 3.5
	465, 3.8
	468, 4.0
6.4	388, 7.9, 17t, #16, T-200A-6
6.7	219, 7.9, 35t, #24, broken, T-50-2, epoxied, 2p38, see 5.9 & 6.4
7.0	197, 7.9, 35t, #28, T-44-2, 3p2
7.2	263, 7.9, 21t+lead, #18, T-225-2
7.3	172, 9, 40t, #28, T-37-2, 3p83
	223, 3.5
	258, 5.4
7.3	254, 7.9, 40t, #28, T-50-7, tap at 10t, 2p39, see 8.2
7.4	265, 7.9, 22t+lead, #18, T-225-2
	415, 3.5
	415, 3.6
	415, 4.0
	352, 7.1
7.5	323, 7.9, 31t, #18, T-94-6, 1p126
8.0	201, 7.9, 38t, #28, T-44-6, 3p2
8.0	258, 7.9, 23t, #18, T-225-2
	202, 3.5
	228, 5.4
	238, 7.0
8.2	237, 7.9, 40t, #28, T-50-7, tap at 10t, 2p39, see 7.3
	232, 10.1
	411, 3.5
	411, 3.6
	410, 3.8
	408, 4.0
9.5	282, 7.9, 27t, #16, T-200-6, 2p66
	212, 7.1
9.5	200, 7.9, 42t, #26, T-50-2, 1p131
	170, 10.1
9.8	192, 7.9, 43t, #26, T-50-2, 1p131
10.5	195, 7.9, 44t, #26, T-50-2, 1p131
11.35	166, 2.52, 52t, #30, T-37-2, 2p4
	174, 7.05
11.9	166, 7.9, 52t, #30, T-37-2, 2p4
12.0	203, 2.52, 53t, T-50-6
12.1	195, 2.52, 53t, T-50-6, w/crossover, in, winding
12.9	181, 2.52, 48t, #28, T-50-2, 3p52